Article

Current Biology

Tissue-Autonomous Phenylpropanoid Production Is Essential for Establishment of Root Barriers

Graphical Abstract

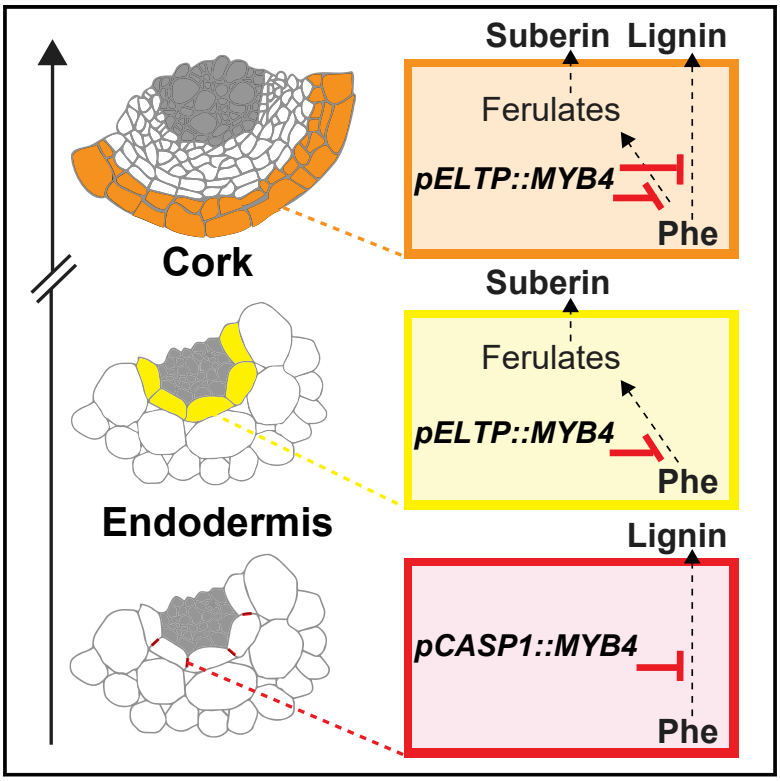

Highlights

- Autonomous production of phenylpropanoids is required for Casparian strip formation
- Phenylpropanoids are essential for suberin deposition in endodermis and cork
- Cork differentiation requires autonomous production of phenylpropanoids
- Spatiotemporal repression of phenylpropanoids can dissect barrier functions

Authors

Tonni Grube Andersen, David Molina, Joachim Kilian, Rochus B. Franke, Laura Ragni, Niko Geldner

Correspondence

tandersen@mpipz.mpg.de (T.G.A.), laura.ragni@zmbp.uni-tuebingen.de (L.R.), niko.geldner@unil.ch (N.G.)

In Brief

Andersen et al. show here that cell-autonomous phenylpropanoid production is required for root barrier formation and integrity.

Andersen et al., 2021, Current Biology *31*, 965–977
March 8, 2021
https://doi.org/10.1016/j.cub.2020.11.070

CellPress

Current Biology

CellPress

Article

Tissue-Autonomous Phenylpropanoid Production Is Essential for Establishment of Root Barriers

Tonni Grube Andersen,[1,5,4,*] David Molina,[2] Joachim Kilian,[2] Rochus B. Franke,[3] Laura Ragni,[2,*] and Niko Geldner[1,*]
[1]Department of Plant Molecular Biology, University of Lausanne, 1015 Lausanne, Switzerland
[2]ZMBP—Center for Plant Molecular Biology, University of Tuebingen, Auf der Morgenstelle 32, 72076 Tuebingen, Germany
[3]Institute of Cellular and Molecular Botany, Rheinische Friedrich-Wilhelms-University of Bonn, Kirschallee 1, 53115 Bonn, Germany
[4]Present address: Max Planck Institute for Plant Breeding Research, Carl-Von-Linné-weg 10, 50829 Cologne, Germany
[5]Lead Contact
*Correspondence: tandersen@mpipz.mpg.de (T.G.A.), laura.ragni@zmbp.uni-tuebingen.de (L.R.), niko.geldner@unil.ch (N.G.)
https://doi.org/10.1016/j.cub.2020.11.070

SUMMARY

Plants deposit hydrophobic polymers, such as lignin or suberin, in their root cell walls to protect inner tissues and facilitate selective uptake of solutes. Insights into how individual root tissues contribute to polymer formation are important for elucidation of ultrastructure, function, and development of these protective barriers. Although the pathways responsible for production of the barrier constituents are established, our models lack spatiotemporal resolution—especially in roots—thus, the source of monomeric barrier components is not clear. This is mainly due to our restricted ability to manipulate synthesis of the broadly important phenylpropanoid pathway, as mutants in this pathway display lethal or pleiotropic phenotypes. Here, we overcome this challenge by exploiting highly controlled *in vivo* repression systems. We provide strong evidence that autonomous production of phenylpropanoids is essential for establishment of the endodermal Casparian strip as well as adherence of the suberin matrix to the cell wall of endodermis and cork. Our work highlights that, in roots, the phenylpropanoid pathway is under tight spatiotemporal control and serves distinct roles in barrier formation across tissues and developmental zones. This becomes evident in the late endodermis, where repression of phenylpropanoid production leads to active removal of suberin in pre-suberized cells, indicating that endodermal suberin depositions might embody a steady state between continuous synthesis and degradation.

INTRODUCTION

Among the diffusion barriers in root cell walls, the best characterized is, arguably, the Casparian strip (CS). The CS consists of precisely localized oxidatively coupled lignin-polymer depositions between the newly differentiated endodermal cells.[1,2] As development progresses, the surface of most endodermal cells becomes covered by hydrophobic suberin (Figure 1A).[3] In contrast to the CS, the suberin barrier consists of lamellae-like structures below the primary cell wall,[4,5] constituting a transmembrane rather than an apoplastic barrier,[6–8] i.e., blocking uptake into cells. The exact lamellae structure remains enigmatic but consists of a crosslinked matrix of fatty acids, glycerol, and aromatic monomers joined through a variety of ester and oxidative couplings.[9,10] Establishment and function of endodermal barriers is tightly controlled by a surveillance system.[11] This consists of an elegant, localized multi-component pathway,[12] which requires diffusion of Casparian strip integrity factor (CIF) peptides from the stele to the surface of the endodermis. Here, CIF peptides activate the leucine rich repeat (LRR)-family receptor SCHENGEN 3 (SGN3)[13] (also called GSO1).[14] This creates a self-regulating system, as formation of a tight CS inhibits CIF diffusion. In the case of a non-functional CS, excess activation of this pathway serves to initiate endodermal "sealing" through ectopic non-CS localized lignification and suberin depositions in the younger, normally unsuberized endodermal cells.[15]

In the older part of the root, radial cell divisions in the stele lead to thickening of the root (secondary growth). As a consequence, the endodermis undergoes programmed cell death, the outer cell layers are shed, and the barrier function is overtaken by the periderm.[17] The periderm consists of the meristematic phellogen (originating from the pericycle), which divides bifacially and gives rise to cork (toward the soil) and phelloderm layers (toward the vasculature).[18] Cork cell walls are highly suberized and lignified, which is essential for their barrier role. In line with this, elevated number of cork layers and suberin content have been associated with increased tolerance to stresses.[18–21]

Common to the polymeric root barriers across these developmental stages and tissues is that their building blocks are derived from the fatty acid (aliphatic) and phenylpropanoid (PP) (aromatic) pathways. For production of aliphatic suberin constituents, fatty acids are oxidized[22,23] and conjugated to glycerol moieties via glycerol-3-phosphate acyltransferases (GPATs)[24–26] before export to the apoplast. Suberin biosynthetic gene expression correlates with suberin deposition,[17,27] and *GPAT5* has been established as a marker for endodermal cells undergoing suberization.[28] Therefore, combined with the hydrophobic nature of fatty acids, it is reasonable to assume that aliphatic constituents of

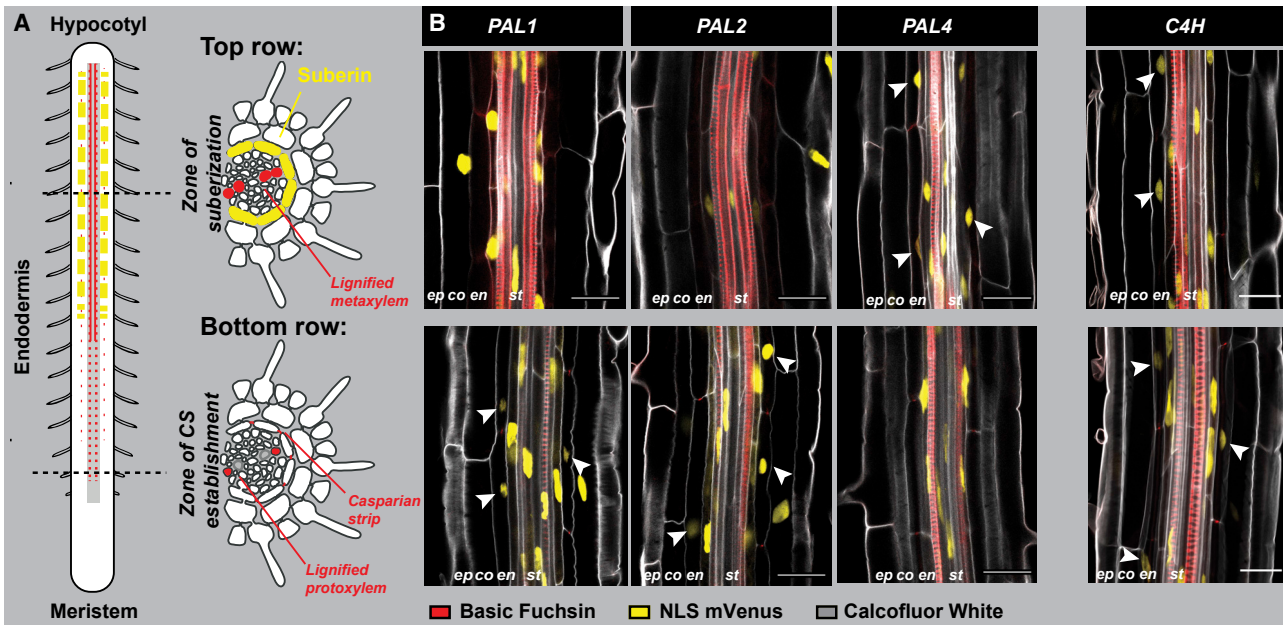

Figure 1. Essential Phenylpropanoid Pathway Genes Are Expressed in the Root Endodermis

(A) Endodermis differentiation can be divided in two successive steps: first, Casparian strips (CSs) are deposited (zone of CS establishment) concomitantly with protoxylem lignification. Second, the suberin lamella is formed (zone of suberization) alongside metaxylem lignification.

(B) Activity of nuclear localized (NLS) 3× mVenus fusion reporters driven by promoter regions of root-expressed *phenylalanine ammonia lyase* (*PAL*) and *cinnamate 4-hydroxylase* (*C4H*) homologs in *Arabidopsis* roots. Expression in 5-day-old roots in the zone of CS establishment (bottom) and suberization (top) of the endodermis is shown. All roots were fixed using a previously established ClearSee protocol.[16] Cell walls were highlighted using Calcofluor White, whereas basic fuchsin was used to highlight lignin depositions in the xylem and in the CSs. Arrowheads point to endodermis cells with reporter activity. co, cortex; en, endodermis; ep, epidermis; st, stele. Scale bars represent 25 μm.

suberin are produced by the depositing tissues themselves.[3] In contrast, the source tissue for PP-derived barrier constituents is less clear, as these have the physio-chemical properties for diffusion across tissues.[29] Besides acting as structural constituents, such as coniferyl alcohol (lignin) and ferulic acid (FA) (suberin), the PP pathway gives rise to a bouquet of metabolites that function in different chemical systems. These include defenses, chelators, colorants, and/or pollinator attractors.[30] Phenylalanine is the major precursor for PPs in most plants, and the initial two committing steps of the PP pathway are catalyzed by the phenylalanine ammonia lyase (PAL)[31] and cinnamate-4-hydroxylase (C4H) enzymes, respectively.[32–34] However, a large degree of redundancy, multi-gene families, and promiscuous branch-point enzymes make it difficult to pinpoint the exact origin of a given PP metabolite. An additional issue is that barrier precursors needed for polymerization and deposition in the cell walls must be transported across the plasma membrane to reach the apoplast. Therefore, the origin of these metabolites is even more enigmatic, as they can be produced and employed cell autonomously or originate from distal cells. Indeed, in the xylem, both cell-autonomous and distal PP production for lignin monomers occurs.[35] Despite the importance of PP metabolites for barriers, and the close proximity of the barrier-containing tissues to the xylem, the tissue-specific coordination of the PP synthesis remains unclear.

Here, we address this question in the roots of *Arabidopsis*. By employing transcriptional repressors in a tissue- and time-dependent manner, we created plants with controllable reduction in PP synthesis within discrete, tissue-specific subzones of the root. This allowed us to investigate the origin of PP precursors and the functional role in different root barriers across root development. We show that both endodermis and cork have the capacity to synthesize PP-derived metabolites. Moreover, our controlled manipulations allowed us to establish that the PP metabolites serve distinct, overlooked functions in barrier dynamics and adherence to the cell wall, especially with regards to endodermal suberin.

RESULTS

Endodermal Cells Have the Capacity for PP Synthesis

To establish whether the endodermis has the capacity to synthesize PP-derived metabolites, we investigated the expression of the PP pathway in *Arabidopsis* roots. *Arabidopsis* has 4 homologs of the *PAL* genes,[36] where only *PAL1*, *PAL2*, and *PAL4* transcripts can be detected in roots.[37] In contrast, only one *C4H* locus exists.[36] As publicly available datasets do not provide sufficient resolution for our analysis, we constructed fluorescent, transcriptional reporters based on promoter regions of *PAL1*, *PAL2*, *PAL4*, and *C4H* driving expression of a nuclear-localized triple mVenus reporter (NLS 3× mVenus). We investigated expression of these reporters at two critical endodermal developmental stages: (1) during CS establishment, which occurs simultaneously to protoxylem lignification (Figure 1A, bottom panel) and (2) during suberization, which happens concomitantly to metaxylem lignification (Figure 1A, top panel). Expectedly, in

roots of 5-day-old seedlings, activity of all promoters was found within the vasculature/stele at both developmental stages (Figure 1B) where the PP pathway is presumably responsible for synthesis of lignin monomers for xylem formation. We also found evidence for expression of PP genes in the cortex (Figure 1B), which might be due to the formation of other PP-derived metabolites, such as coumarins,[38] in this tissue. *PAL1* and *PAL2* promoters were additionally active in the zone of CS establishment (Figure 1B, bottom panel). Interestingly, *PAL4* was only found to be endodermis expressed in the zone of suberization (Figure 1B, top panel). *C4H* expression was broader and encompassed the cortex, endodermis, and stele at both investigated stages (Figure 1B). Thus, the endodermis expresses key genes of the PP pathway, which makes it plausible that this layer can produce PP metabolites.

Lignification of CS and Xylem after Inhibition Recovers with Similar Dynamics

Lignification of the CS and xylem starts at a similar developmental point in the root, which suggests that these processes share a common source of PP substrates. Our next step was therefore to address whether lignin deposition in the CS and xylem is coordinated. As previously described, treating 5-day-old *Arabidopsis* seedlings for 24 h with the C4H-inhibitor piperonylic acid (PA)[39] leads to a non-lignified zone where developing xylem and CS would normally have initiated lignification (Figure 2A).[40] To investigate the ability of the tissues to recover lignification after inhibition, we transferred PA-inhibited seedlings to recovery plates (without PA), in presence or absence of the lignin monomer coniferyl alcohol (G-OH) and measured recovery of lignification over time. Lignin deposition without exogenous monomer supply—dependent on endogenous PP synthesis—reoccurred surprisingly fast, as we observed a significant ($p < 0.01$; two-tailed Student's t test versus untreated) lignin-specific fluorescence (basic fuchsin stain) for both the xylem and CS in the PA-induced non-lignified zone after only 4 h of transfer to plates without G-OH (Figures 2B and S1A). This was further decreased by at least 2 h for both CS and xylem in presence of 20 μM G-OH (Figures 2B and S1A). Thus, PA interferes with endogenous monolignol availability, but not apoplastic polymerization capacity, for lignin. Only in the presence of externally supplied G-OH did both xylem and CS fully recover within the tested time frame (Figure 2B). We conclud that lignin polymerization capacity in both the CS and xylem can be uncoupled from substrate availability and that these tissues show similar lignification dynamics (Figures 2B and S1A).

Inhibition of PP Synthesis Leads to Aberrant Suberin Deposition

Disruption of the CS promotes ectopic suberization in young parts of the endodermis due to stimulation of the SCHENGEN (SGN) pathway.[11–13] With this in mind, our PA-inhibited plants must show SGN-dependent responses, such as ectopic suberization (Figure 2A). On a gene expression level, this was indeed the case, as the PA treatment led to a strong upregulation of genes related to suberin biosynthesis in a SGN3-dependent manner (Figure 2C). We realized that we could use this setup to address whether *de novo* deposition of endodermal suberin can occur without the ability to locally produce PP-derived metabolites. Under standard growth conditions, endodermal suberization is initiated in a "patchy" manner (Figures 2A and S1D) as cells at the xylem pole show delay in suberin onset.[28] Intriguingly, in contrast to the normal "smooth" signal observed when staining the endodermal cells with Fluorol Yellow (FY),[40] PA-treated roots showed a "droplet-like" FY signal specifically in the non-lignified zone (Figures 2F, 2G, and S1E). This signal depends on a stimulated SGN pathway, because we did not observe this in PA-treated *sgn3* roots (Figures 2D and 2F). Moreover, in PA-treated roots, suberin depositions already established before the treatment start were strongly reduced in a SGN-independent manner (Figures 2D and 2F) and not due to growth-related changes in the proportions of suberized root zones (Figure S1F). This observation is remarkable and suggests that already established endodermal suberin lamellae are unstable without active PP synthesis. We attempted to identify the specific metabolite involved in this by complementing the PA treatment with PP metabolites typical for lignin and suberin. Intriguingly, only FA and not G-OH in the media led to complementation of the droplet-like ectopic suberin deposition and prevented suberin disappearance in the pre-established zone (Figure 2E). This complementation could not be observed with other FA-related PP acids (Figure S1B). FA is a well-described constituent of suberin, and we therefore investigated a mutant with a non-functional version of the ALIPHATIC SUBERIN FERULOYL TRANSFERASE (ASFT), involved in the incorporation of ferulates into suberin.[27] Transfer DNA (T-DNA) knockout (KO) alleles of this mutant also showed droplet-like suberin depositions in the endodermis, even under normal growth conditions (Figures 2E and S1C). Moreover, FA-dependent complementation was absent in the *asft-1* mutant (Figure 2E). We therefore conclude that a tight coordination of aromatic (in particular FA) and aliphatic monomer synthesis is necessary for correct establishment of the endodermal suberin barrier.

Monolignol Production in the Endodermis Is Required for CS Formation

PA treatment indiscriminately inhibits the PP pathway in all cell types. Thus, we sought to create a genetic tool that would allow tissue-specific repression of PP synthesis, avoiding pleiotropic effects due to disruption of xylem formation, for example. Transcriptional regulation of PP synthesis includes the ethylene-responsive element binding factor-associated amphiphilic repression (EAR) domain-containing subgroup 4 MYB transcription factors.[41] All members in *Arabidopsis* (MYB3, MYB4, MYB7, and MYB32) repress genes of the PP pathway and could in theory work as genetic PP-synthesis repressors through ectopic expression. Although MYB7 represses mainly flavanol biosynthesis,[42] MYB3, MYB4, and MYB32 target expression of *C4H*. It is not clear whether these factors directly repress PP genes, so we focused on MYB4, as its DNA-binding domain has been shown to be required for repression of *C4H*[41] and has recently been shown to additionally repress the final step of phenyl alanine synthesis.[43] We established plant lines containing *MYB4* driven by the promoters of the Casparian strip membrane protein 1 (p*CASP1*)[44] or endodermal lipid transfer protein (p*ELTP*)[7] active specifically in the zone of CS establishment or suberization, respectively (Figure 3A). Consistent with expectations, only plants with p*CASP1*-driven expression of *MYB4* showed CS dysfunction. This was manifested as a "discontinuous" CS with

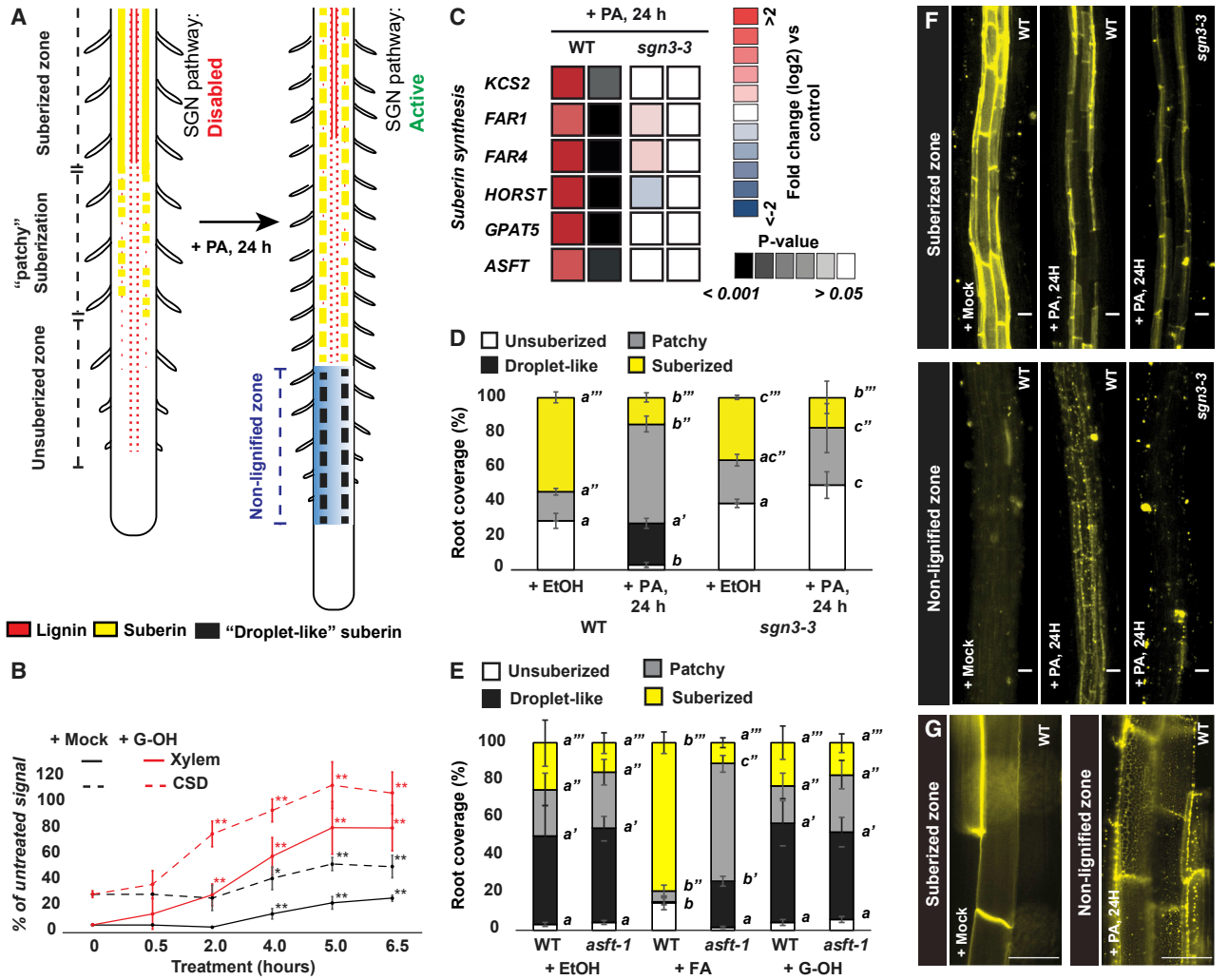

Figure 2. Endodermal Suberin Deposition Is Disrupted by Inhibition of PP Synthesis and Specifically Complemented by Ferulic Acid

(A) Scheme explaining the effects of piperonylic acid (PA) treatment on roots. Roots continue growth during PA treatment, which leads to establishment of a non-lignified zone where the xylem and Casparian strip (CS) are normally lignified in mock conditions. Absence of lignification in the CS domain (CSD) leads to diffusion of CS integrity factor peptides (CIFs) and consecutive activation of the Schengen (SGN) pathway. Activation of the SGN pathway is known to induce ectopic suberization of the otherwise non-lignified endodermal cells.[15] Our experimental setup therefore allowed us to study the effect of inhibited PP-metabolite production on ectopic suberin deposition.

(B) Time course analysis of basic fuchsin signal recovery in the PA-induced non-lignified zone of xylem or CSD. 5-day-old plants were treated for 24 h with PA and then moved to recovery plates with either a mock solution or 20 μM coniferyl alcohol (G-OH) at the indicated time points. The signals were normalized to identically grown non-PA-treated plants. n = 5; *p < 0.05; **p < 0.01; two-tailed Student's t test versus 0 h treatment.

(C) Relative expression of suberin biosynthesis genes in WT and *sgn3-3* roots treated with mock or PA for 24 h. Data were obtained by qPCR as described in the STAR Methods section. For primer and gene information, see Table S1. p values are based on a two-tailed Student's t test versus non-PA-treated control plants of the same genotype.

(D) Quantification of suberin root coverage by Fluorol Yellow (FY) staining of suberin in the endodermis of 5-day-old WT and *sgn3-3* roots treated with mock (EtOH) or PA for 24 h before staining. In the non-lignified zone of PA-treated roots, FY staining gave rise to "droplet-like" structures as seen in (F) and (G); n = 6.

(E) Quantification of suberin root coverage by FY staining in the endodermis of 5-day-old PA-treated WT and *asft-1* mutant roots co-treated with mock (EtOH) or 20 μM ferulic acid (FA) or 20 μM G-OH for 24 h; n = 6.

(F) Representative images of FY staining of the experiment shown in (D). Upper panels correspond to images taken at the level of the suberized zone, whereas lower panels correspond to images taken in non-lignified zone.

(G) Magnification of FY-staining images of a WT mock and PA-treated root in the suberin zone to highlight the suberin droplet-like phenotype shown in (F).

All error bars are SD; letters refer to individual groups/treatments in a one-way ANOVA analysis with a post hoc multiple group t test (Tukey) (p < 0.05). Scale bars represent 25 μm. See also Figure S1.

irregular patches (Figure 3A) and by increased propidium iodide (PI) permeability (Figure 3B). MYB3 and MYB32 showed similar effects, whereas no effects on CS formation was seen when MYB7 was employed in a similar manner (Figure S2D). Importantly, the MYB4-dependent CS disruption could be complemented by addition of G-OH to the media or through expression

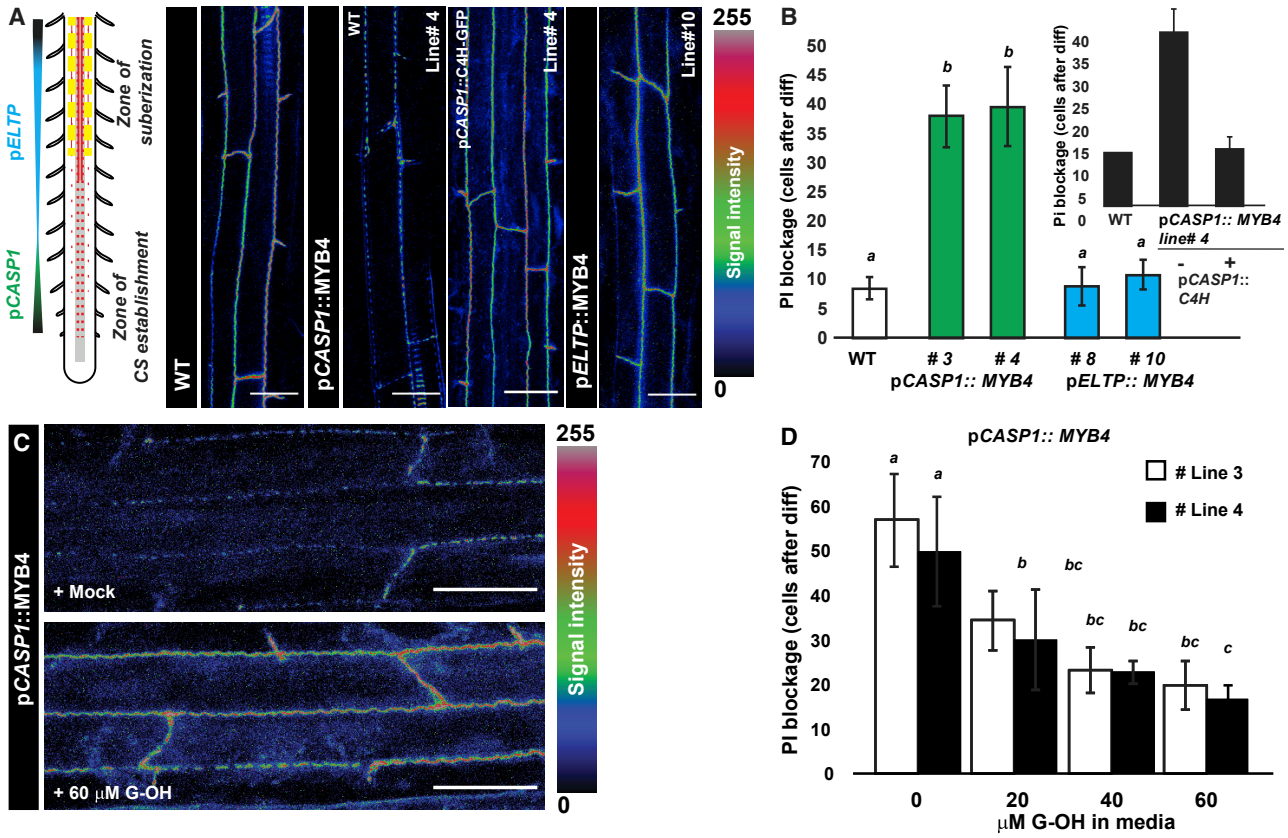

Figure 3. Endodermis-Specific Expression of MYB4 Alters Lignin Deposition and CS Formation

(A) The phenylpropanoid-repressive transcription factor MYB4[41] or cinnamate-4-hydroxylase (C4H) was expressed using the promoter from the CS membrane domain protein 1 (p*CASP1*)[44] active in the endodermis during CS establishment. MYB4 was additionally expressed under the promoter from the endodermal lipid transfer protein (p*ELTP*)[7] active in the zone of suberization. The panels show longitudinal surface projections of lignin depositions in the endodermis stained by basic fuchsin using an established ClearSee-based protocol.[16]

(B) Functional analysis of CS by measuring onset of propidium iodide (PI) diffusion blockage into the stele;[40] n = 6.

(C) Surface view of endodermal CS stained by basic fuchsin in p*CASP1::*MYB4 plants treated with either ethanol (mock) or G-OH upon germination.

(D) Blockage of PI in p*CASP1::*MYB4 roots under increasing amount of G-OH. Plants were germinated and grown for 5 days in presence of the indicated substrate before measurement of PI penetration. n = 6.

All error bars are SD; letters refer to individual groups in a one-way ANOVA analysis with a post hoc multiple group t test (Tukey) ($p < 0.05$). Scale bars represent 10 μm. See also Figure S2.

of *C4H* under the p*CASP1* promoter in p*CASP1::*MYB4-expressing plants (Figures 3B–3D). Together, this strongly suggests that the effect of MYB4 is due to PP synthesis inhibition and not due to a more general interruption of endodermal differentiation, e.g., interference with MYB36 activity.[45,46] Furthermore, plants with ectopic MYB4 expression in the differentiating endodermis showed correct localization of the CS protein CASP1 (Figure S2C).[2] We did not find differences in root length for all lines compared to wild type (WT), even though we did observe a trend toward shorter roots in plants with ectopic MYB expression (Figure S2B). As the employed promoters are not active in the meristematic zone of roots, this probably reflects physiological effects of disrupted barrier formation. None of the investigated lines led to decreased lignin signal in the xylem (Figure S2E).

The remaining CS-associated lignin observed in p*CASP1::*MYB4 plants could be explained by PP synthesis in adjacent tissues and/or by ectopic lignification activated by the SGN surveillance system.[15] To address this, we created plants with p*CASP1*-driven MYB4 expression in the *sgn3-3* background.[13] Interestingly, only this background led to a significant decrease of *C4H* expression (Figure 4A), suggesting that activation of *C4H* by the SGN pathway might overshadow the relatively restricted tissue-specific repression caused by MYB4 under the *CASP1* promoter. To test this, we combined expression of the p*CASP1::*MYB4 construct with the p*C4H::*NLS 3× mVenus reporter. In these plants, *C4H* reporter activity was strongly decreased in the endodermis, although at least the cortex showed significantly increased *C4H* activity ($p < 0.05$) when normalized to WT (Figures 4B and S2F). Moreover, we found that externally applied CIF2 peptide, which is a ligand for the SGN3 receptor,[11] could induce activity of the *C4H* transcriptional reporter across all tissue layers, but only in plants with an active SGN pathway (Figures 4C and S2G). Taking together, SGN-activated lignin production/secretion from the endodermis-adjacent tissues appears to contribute to ectopic endodermis lignification. To substantiate this, we expressed a p*CASP1::*MYB4-GFP construct in a *cif1cif2*

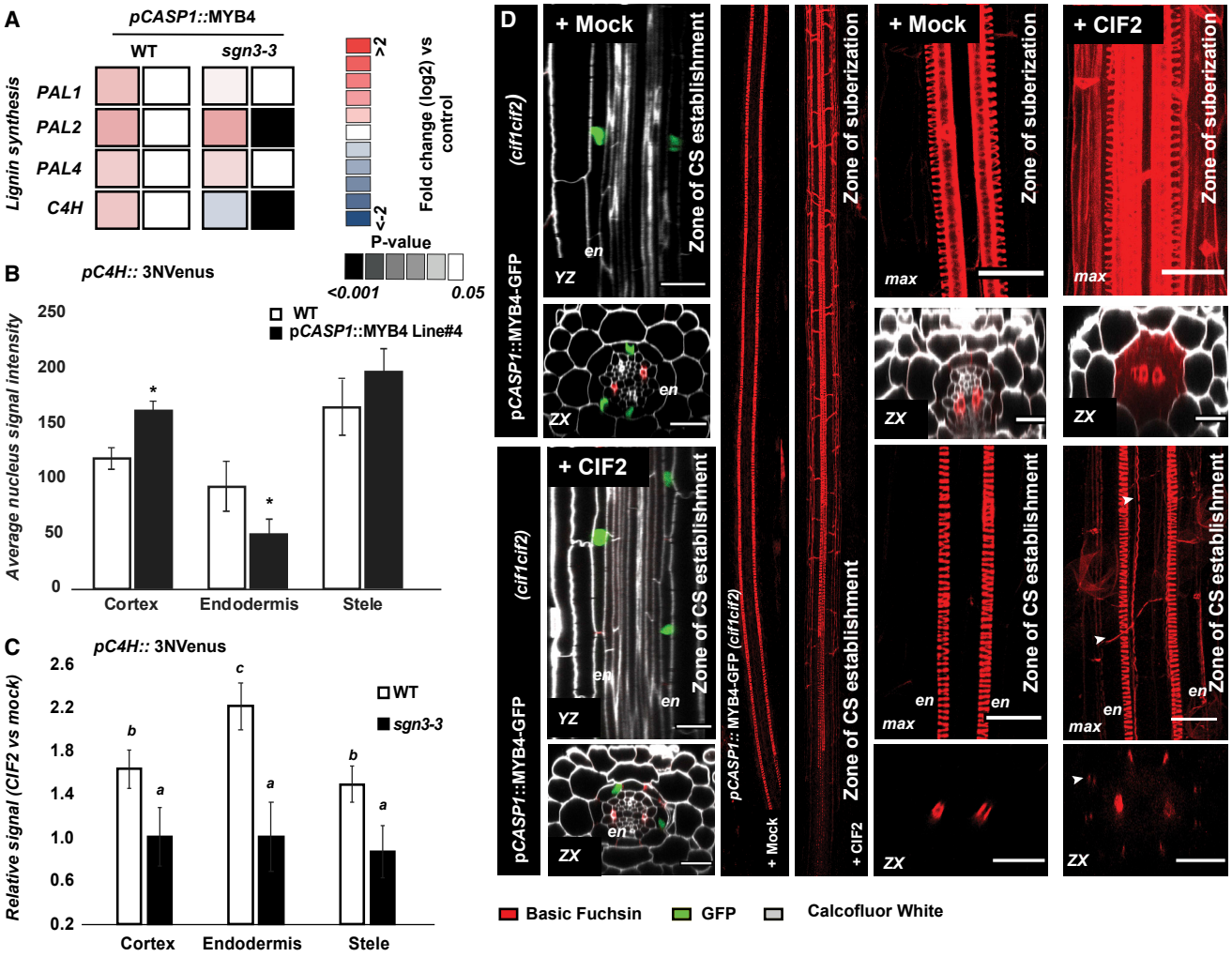

Figure 4. Compensatory SGN3-Dependent Lignification Is Activated upon MYB4 Expression in the Endodermis

(A) Relative expression of genes involved in the phenylpropanoid (PP) pathway in 5-day-old WT and *sgn3-3* roots expressing p*CASP1::*MYB4 measured by qPCR. Expression was normalized to each genotype without MYB4 expression. n = 3; p values are based on a two-tailed Student's t test (PA versus mock treated). For primer and gene information, see Table S1.

(B) Average fluorescence signal of *C4H* activity (p*C4H::*3NVenus) in 5-day-old WT and p*CASP1*::MYB4 roots. n = 5.

(C) Relative quantification of *C4H* activity (p*C4H::*3NVenus) in the zone of CS establishment in WT and *sgn3-3* mutants treated with CIF2 peptide. Fluorescent intensity signals were normalized to mock-treated roots of the same line. All treatments were 24 h. n = 8.

(D) Longitudinal YZ, XZ, or maximum projections of lignin deposition (basic fuchsin staining) in the endodermis (both CS establishment and suberization zones) and vasculature of 5-day-old seedlings p*CASP1*::MYB4-GFP *cif1cif2* roots upon treatment with mock or 1 μM CIF2 peptide for 24 h. Roots were fixed and stained with Calcofluor White and basic fuchsin.[16] Arrowheads point to non-connected lignification; max, maximum projection.

All error bars are SD; scale bars represent 10 μm. Letters refer to individual groups in a one-way ANOVA analysis with a post hoc multiple group t test (Tukey) ($p < 0.05$).

double mutant, which knocks out root ligands for the SGN pathway and phenocopies *sgn3* but allows the activation by addition of CIF peptides to the media.[11] When grown under mock conditions, these lines lacked lignin across the entire endodermis, although CIF2 treatment led to non-connected endodermal lignin depositions in both the zone of CS establishment and in the suberizing zone (Figure 4D). Thus, under normal conditions, the endodermis autonomously produces lignin monomers required for CS formation without dependency on synthesis from surrounding tissues. Upon barrier disruption, ectopic lignification is likely to be coordinated with the adjacent tissues through SGN-dependent activation of monolignol production.

Continuous PP Synthesis in the Endodermis Is Essential for Suberization

Besides the defective CS, all the p*CASP1::*MYBs lines had suberin deposition patterns similar to those of WT plants (Figures 5A, 5B, S2A, S2D, and S3B). This is intriguing, as the endodermis in the CS-establishing zone should undergo suberization due to activation of the SGN pathway. These plants also displayed a reduced suberin deposition response to the CIF2 peptide (Figure S3B). One explanation for this is that the presence of MYB4 in the endodermis represses suberin deposition. In line with this, plants expressing MYB4 in the zone of suberization (p*ELTP* promoter) had normal CSs (Figure 3A) but displayed an almost complete

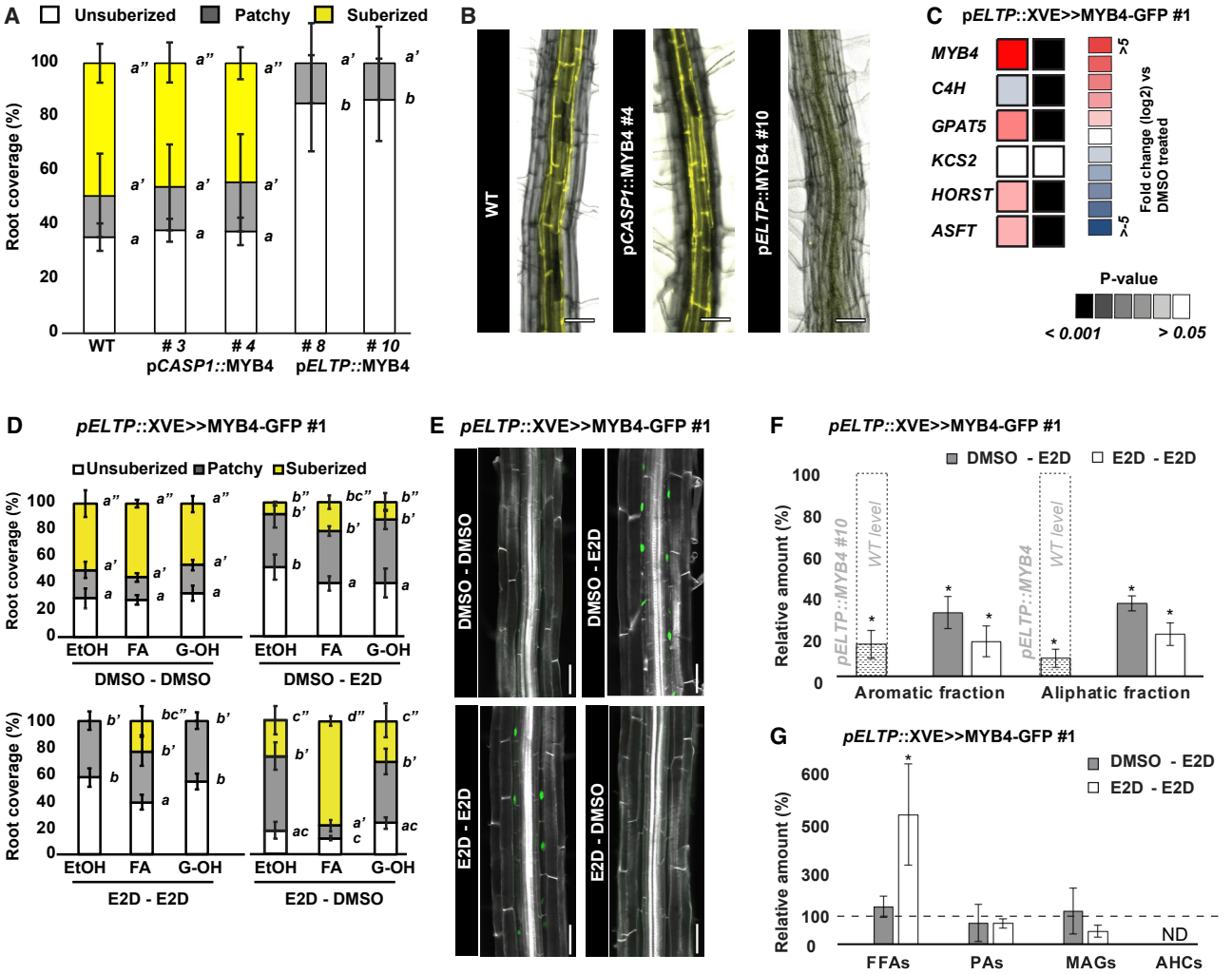

Figure 5. Repression of PP Synthesis in the Mature Endodermis Leads to Suberin Detachment

(A) Quantification of relative suberin root coverage by FY staining in the endodermis of 5-day-old roots; n = 6.

(B) Representative images of FY-stained, 5-day-old root quantified in (A). Scale bars represent 25 μm.

(C) Relative expression of suberin biosynthetic genes in the endodermis upon induction of p*ELTP::*XVE>>MYB4-GFP measured by qPCR. Expression was normalized to DMSO-treated plants. n = 3; p values are based on a two-tailed Student's t test (PA versus mock treated). For primer and gene information, see Table S1.

(D) Quantification of suberin root coverage by FY staining. p*ELTP::*XVE>>MYB4-GFP plants were grown for 4 days on either DMSO- (upper graphs) or 5 μM E2D (lower graphs)-containing media and then transferred to plates containing E2D or DMSO, respectively, in combination with ethanol (EtOH), 20 μM FA, or 20 μM G-OH for 2 days before suberin quantification by FY staining.

(E) GFP signal in 6-day-old p*ELTP::*XVE>>MYB4-GFP plants grown on plates containing DMSO or 5 μM E2D. Scale bars represent 50 μm.

(F) Relative amount (%) of suberin aromatic and aliphatic fractions from 8-day-old *pELTP::*MYB4 or p*ELTP::*XVE>>MYB4-GFP roots grown under E2D regimens (6 days mock + 2 days E2D: "DMSO-E2D" or 6 days E2D + 2 days E2D: "E2D-E2D"). Levels were normalized to WT plants of identical age for p*ELTP::*MYB4 (white with stripes) and to DMSO-DMSO-treated plants for p*ELTP::*XVE>>MYB4-GFP (gray, white), respectively; n = 3–5; *p < 0.05; two-tailed t test versus WT or mock.

(G) Relative amount (%) of chloroform extractives of the endodermis of 18-day-old p*ELTP::*XVE>>MYB4-GFP-expressing roots under different E2D treatments (2-day, DMSO-E2D or 18-day, E2D-E2D); n = 3–4; *p < 0.05; two-tailed t test versus mock.

AHCs, alkyl hydroxycinnamates; FFAs, free fatty acids; MAGs, monoacylglycerol conjugates; ND, not detected; PAs, primary alcohols; WT, wild type. All error bars are SD. Letters refer to individual groups in a one-way ANOVA analysis with a post hoc multiple group t test (Tukey) (p < 0.05). See also Figures S2–S4.

loss of FY-stained endodermal cells (Figures 5A and 5B). MYB3 or MYB32 had a similar effect, whereas no decrease in suberin signal was seen in p*ELTP::*MYB7-expressing plants (Figures S2A and S2D). p*ELTP::*MYB4 roots showed a strong decrease in all major aromatic and aliphatic suberin constituents compared to WT (Figures 5F and S4A), confirming that ectopic MYB4 expression indeed represses suberin in the endodermis. Next, we investigated whether the negative effects of MYB4 on suberin deposition can be explained by repression of suberin biosynthesis genes. To address this, we employed an estradiol (E2D)-inducible chimeric transcription activator based on fusion of the DNA-binding domain of the bacterial repressor LexA (X), the acidic transactivating domain of VP16 (V), and the regulatory region of the human estrogen receptor (E; ER) (XVE) containing the p*ELTP*[47] promoter

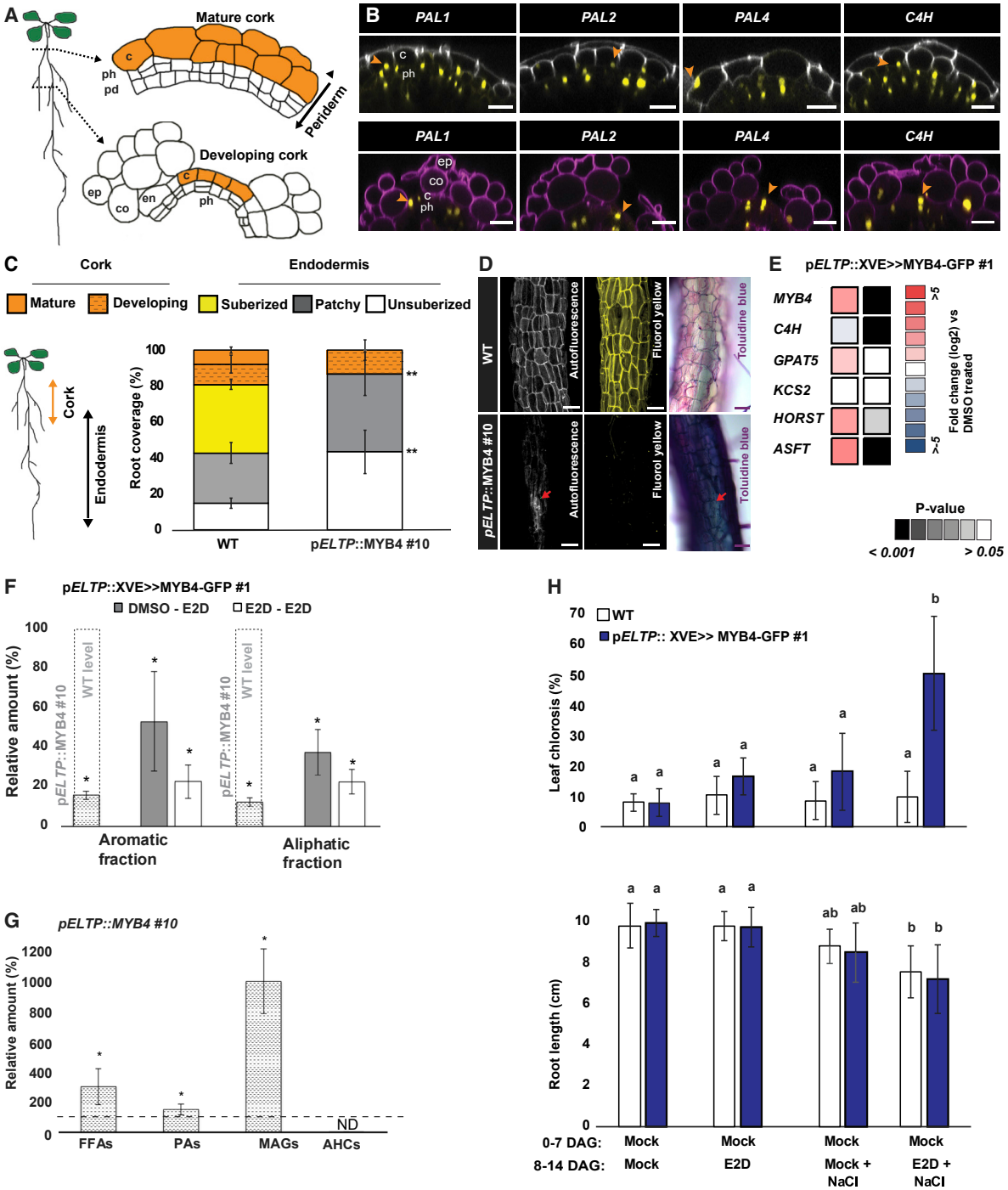

Figure 6. Collapse of Cork Formation by Ectopic Expression of MYB4 in the Periderm

(A) A simplified scheme of periderm development in the *Arabidopsis* root. During secondary growth, the root increases in girth, the endodermis undergoes programmed cell death, and its barrier function is eventually replaced by the periderm.[17,18] This is a developmental process, and zones of "developing" and "mature" cork formation can be identified along the root.

(B) Activity of nuclear localized (NLS) 3× mVenus fusion reporters driven by promoter regions of root-expressed *PAL* and *C4H* homologs in 21-day-old *Arabidopsis* roots at the different cork developmental stages (orange arrowheads). Cell walls were highlighted using the intrinsic autofluorescence of cork cells (gray) in the mature cork zone or PI (magenta) for "patchy" cork zones. Orange arrowheads point toward cork cells with positive marker expression.

(C) Quantification of suberin root coverage in 12-day-old WT and p*ELTP*::MYB4 roots using FY staining[28] (n = 6; *p < 0.05; **p < 0.01; two-tailed Student's t test versus WT).

(D) Autofluorescence (left panel), FY staining (middle panel), and toluidine blue (right panel) of cork cells in WT and p*ELTP*::MYB4 19-day-old roots.

(legend continued on next page)

to add temporal control to the MYB4 expression. We used this system to drive a MYB4-GFP fusion (p*ELTP*::XVE>>MYB4-GFP). The fusion of MYB4 to GFP had no effect on the repressive effect of MYB4 on suberin (Figure S3C). Interestingly, when roots were subject to 48 h of E2D exposure, we saw a significant increase in expression of several key genes for aliphatic suberin constituent synthesis as well as a concomitant repression of *C4H* (Figure 5C). Thus, the repressive effects of MYB4 on suberin deposition are not due to direct transcriptional repression of the underlying biosynthesis of aliphatic monomers. To further establish whether the disappearance of suberin can be complemented by PP-derived metabolites, seedlings were grown for 4 days on mock- or E2D-containing plates and transferred to similar plates with or without PP metabolites for 2 days. After a total of 6 days E2D induction, in control treatments (2 days of EtOH), the suberized zone was strongly reduced when compared to similar non-induced plants (Figure 5D). We could partially complement this by adding FA or other PP-derived acids, but not G-OH, to the media for the last 2 days (Figures 5D and S3A), supporting that active endodermal PP synthesis is necessary to establish a suberized barrier. We then grew plants for 4 days on mock-containing plates to allow a suberized zone to be established (Figure S1F) and transferred to E2D plates (suppressing further PP-metabolite synthesis) for 2 days with or without PP-derived metabolites. Remarkably, and in line with our observations for PA-treated roots (Figures 2D, 2F, and S1F), the proportion of root containing a suberized zone of the root was significantly ($p < 0.05$) reduced when compared to mock-treated plants but was again partially complemented by PP-derived acids (Figures 5D and S3A). The lack of complete complementation by PP acids could be explained by the fact that MYB4 also represses genes of the PP pathway involved in FA-coenzyme A (CoA) conjugation.[41] To further probe this, we reversed the experimental setup and allowed plants to grow for 4 days on E2D-containing plates with 2 additional days on mock-containing plates with or without PP-derived metabolites. This recovery phase allowed complete MYB4-GFP degradation (Figure 5E). Interestingly, after the treatments, roots regained a suberized zone, even in mock treatments (Figure 5D), which was strongly increased by the specific addition of FA to recovery plates (Figures 5D and S3A). In conclusion, the p*ELTP*::XVE>>MYB4-GFP line on suberin deposition recapitulates the effect of both PA treatment and the p*ELTP*::MYB4 line. Therefore, these experiments strongly indicate that suberin is incorrectly attached to the cell wall and removed from the endodermal cell wall matrix upon repression of PP production in the endodermis.

Unbound Aliphatic Suberin Constituents Accumulate in Absence of Aromatics

Constitutive expression (p*ELTP::*MYB4) or short (2-day) or constitutive MYB4 induction using the p*ELTP::*XVE>>MYB4-GFP system led to comparable reductions of both extractable aromatic and aliphatic suberin components when compared to WT or mock treatment, respectively (Figures 5F and S4B). As the suberin biosynthetic machinery was not repressed by MYB4 (Figure 5C), aliphatic constituents were probably not incorporated in the final suberin structure without PP-derived metabolites. To clarify the fate of these metabolites, we performed a chloroform-based extraction[48] of the endodermis-containing root parts during MYB4-GFP induction. Surprisingly, only in continuously induced or constitutive MYB4-expressing plants did the reduction of suberin-associated aromatic components co-occur with a significant overaccumulation of free aliphatic constituents, such as very-long-chain free fatty acids (FFAs), characteristic for suberin ($p < 0.01$; two-tailed Student's t test versus mock; Figures 5G and S4C). Based on this, we propose that, in absence of PP metabolites, aliphatic constituents, meant to be incorporated into the suberin matrix, accumulate as unpolymerized constituents in the apoplast and/or are funneled into other FFA-related pathways.

Repression of PP Synthesis in Periderm Leads to Collapse of the Cork Barrier

To analyze whether suberin depositions in the barrier layers of the periderm behave in a similar manner to the endodermis with regards to PP biosynthesis, we grew plants for up to 21 days to allow secondary growth. The periderm can be divided into a "developing" and a "mature" cork stage dependent on the distance from the meristematic zone (Figure 6A). In both of these zones, we observed activity of all analyzed PP expression reporters in the cork and phellogen layers (Figure 6B), suggesting that the periderm also functions autonomously to produce monomers for construction of the cork barrier. As the *ELTP* promoter is active in the periderm during secondary growth (Figure S5A), we investigated the specific role of PP production in the periderm using our MYB4-based repressor tools. Similar to the endodermis, p*ELTP*::MYB4-expressing plants showed a reduction of lignin and suberin staining of cork cells when compared to WT (Figures 6C, 6D, S5B, and S5C). The reduced suberin content was maintained through periderm development (Figures 6C, 6D, and S5C), indicating that the periderm is dependent on tissue-autonomous PP production in a similar manner to the endodermis. Interestingly, p*ELTP::*MYB4-expressing plants had collapsed cork cells, which compromised the barrier function as visualized

(E) Relative expression of suberin biosynthetic genes in the periderm upon induction of p*ELTP::*XVE>>MYB4-GFP measured by qPCR. Expression was normalized to DMSO-treated plants. n = 3; p values are based on a two-tailed Student's t test (PA versus mock treated). For primer and gene information, see Table S1.

(F) Relative amount (%) of suberin aromatic and aliphatic fractions form the cork of 20-day-old WT, p*ELTP::*MYB4, and p*ELTP*::XVE>>MYB4-GFP roots. Levels were normalized to WT and mock-treated plants of identical age for p*ELTP::*MYB4 and p*ELTP::*XVE>>MYB4-GFP, respectively. n = 3–4; *$p < 0.05$; two-tailed t test versus WT or mock.

(G) Relative amounts (%) of chloroform extractives of 20-day-old p*ELTP*:: MYB4-expressing roots. Normalization was to WT plants of identical age; n = 3; *$p < 0.05$; two-tailed t test versus WT.

(H) Leaf chlorosis (%) and primary root length quantification of WT or p*ELTP::*XVE>>MYB4-GFP plants 7 days after germination (0–7 DAGs) under standard conditions (mock) and transferred for 7 days to plates with combinations of mock, 5 μM E2D, and 100 mM NaCl treatments for an additional 7 days (8–14 DAGs). All error bars are SD. *$p < 0.05$; **$p < 0.01$ in a two-tailed Student's t test versus WT. Letters refer to individual groups in a one-way ANOVA analysis with a post hoc multiple group t test (Tukey) ($p < 0.05$).

c, cork; DAG, days after germination; pd, phelloderm; ph, phellogen. Scale bars represent 20 μm. See also Figures S5–S7.

by increased toluidine-blue penetration (Figure 6D). We therefore employed the p*ELTP::*XVE>>MYB4-GFP system to investigate whether suberin in cork cell layers are dependent on continuous PP synthesis. To ensure onset of cork differentiation, we let the plants grow for 12 days on plates containing either mock or 5 μM E2D and then cross-transferred them to mock or E2D for an additional 8 days to allow constant or induced expression of MYB4-GFP in pre-formed periderm cells. In both cases, we observed cork cell collapse similar to the p*ELTP::*MYB4 plants; however, this appeared to be stronger in plants with constant induction (Figure S5D), which likely reflects that the suberin pre-established in the initial 12 days mock treatment might not be degraded in the periderm. Also in this tissue, we observed that MYB4 led to a transcriptional repression of *C4H* and activation of some of suberin biosynthesis genes (Figure 6E), further indicating that the repressive effect of MYB4 does not affect suberin synthesis directly. To determine the fate of the suberin constituents in the periderm, we isolated the cork-containing root parts and subjected them to the same gas chromatography-mass spectrometry (GC-MS)-based pipeline as the endodermis samples. All lines (including constitutive p*ELTP::*MYB4 plants) displayed a strong reduction in suberin constituents when compared to the respective controls (Figures 6F, S5E, and S6A), supporting that ectopic MYB4 expression prevents *de novo* suberin deposition. Both constant and short-term-induced MYB4-GFP (and constitutive p*ELTP::*MYB4-expressing plants) showed a reduced content of the extractable aliphatic-aromatic conjugated alkyl hydroxycinnamates (AHCs) (Figures 6G, S6B, and S6C). This observation suggests that the detected AHCs originate from the cork. In contrast to the endodermis inductions, where aromatic-conjugated aliphatic compounds are typically found in low levels using the employed extraction method,[48] repression in the periderm led to increased accumulation of aliphatic suberin constituents in the chloroform fractions (Figures 6G, S6B, and S6C). Surprisingly, continuous repression using the XVE system led to a decrease in these components (Figure S6C), which is most likely related to physiological effects of the repressed periderm barrier formation on all plant processes. Finally, to substantiate that ectopic MYB4-GFP expression in the cork and the consequential cell collapse give rise to a non-functional periderm barrier, we grew plants on mock-containing plates for 7 days followed by transfer to mock or 5 μM E2D-containing plates with or without 100 mM NaCl for an additional 7 days. Only the combination of E2D (and the resulting MYB4-GFP expression) and NaCl led to a significant ($p < 0.01$; pairwise t test) increase in leaf chlorosis (Figures 6H and S7A). This supports a role for the periderm in salt stress protection and emphasizes the defective barriers in our analysis. In all cases, NaCl stress led to reduced root lengths, without significant difference between the mock and E2D-treated plants (Figure 6H). In summary, our periderm analysis indicates that, similar to the endodermis, suberin cannot be incorporated correctly into the cork barrier upon ectopic MYB4 expression. Moreover, this highlights our temporally controlled MYB4 expression as a model to study physiological roles of the periderm barrier.

DISCUSSION

Plant apoplastic barriers help to control nutrient uptake, gas exchange, and water availability and confer protection to biotic and abiotic stresses. These structures are therefore traits of crucial agronomical importance. In roots, CSs represent the first apoplastic barrier established after germination. In *Arabidopsis*, polymerization of lignin in the CS occurs few cells after the onset of elongation and simultaneously to xylem differentiation.[2,40] In the xylem, polymerization of lignin can continue after cell death,[49] which indicates that monolignols can diffuse from surrounding cells. Most PPs have the physio-chemical properties to passively diffuse across membranes,[29] which suggests that defining elements of CS lignin originates from xylem, given such a diffusion path already exists for barrier surveillance CIF peptides that are produced in the stele but perceived in the CS domain.[11] In line with this, it is interesting that all of the PP-synthesis genes investigated here showed strong expression in the pericycle (Figure 1B), hinting that this cell layer, situated in between the endodermis and the xylem, may contribute PP metabolites for lignification in both tissues. Moreover, the tight developmental association of lignification dynamics in the xylem and endodermis (Figures 2B and S1A) supports a model where lignification of the distinct, adjacent tissues shares a common biosynthetic framework. Yet, our work clearly demonstrates that, under normal conditions, production of lignin monomers in the endodermis is required for CS formation. Upon CS disruption, the root deposits ectopic non-CS localized lignin in the endodermis through activation of the SGN pathway. Our findings reveal that the PP pathway is responsive to CIF2 treatment in the cortex and stele (Figure 4C). Thus, it is likely that, upon CS disruption, the surrounding tissues aid in ectopic lignification of the endodermis. Indeed, *C4H* was upregulated in these tissues upon MYB4-dependent disruption of the CS (Figure 4B). Although the monolignol-specific ABCG29/PDR1 transporter is expressed in both the vasculature and endodermis,[50] the role of active monolignol transport between root cell types and especially upon SGN activation is still unclear. However, due to the broad range of PP metabolites, tissue-specific compartmentalization—such as production PP metabolites for CS in the endodermis—might add spatial control over metabolites synthesis in a given cell and serve to avoid bottlenecks for compounds produced from a common pool of substrates. In support of this, we observed *PAL4* activity only in the suberizing zone of the endodermis (Figure 1B, top panel), suggesting that this isoform acts in the production of ferulates earmarked for suberin production (Figure 7). Future studies that include careful high-resolution multi-level localization and metabolite analysis of the PP pathway are therefore likely to reveal currently unappreciated regulatory mechanisms that drive tissue and developmental-stage-specific PP metabolic pathways within the root.

Besides the analysis of monolignol production for CS formation, our work reveals an interesting new aspect of suberin behavior, namely that PP-derived metabolites components of the suberin matrix serve to somehow stabilize and anchor the polymers to the cell wall and regulate active turnover of suberin in the endodermis. The length of the suberized endodermal zone is increased or decreased under certain abiotic stresses in an abscisic acid (ABA)- and ethylene-dependent manner, respectively.[7] An active mechanism for turnover of suberin based on regulation of PP metabolism in the endodermis would therefore allow the plant to quickly adjust its diffusion barrier to abiotic changes in the external environment. The PP pathway is responsive to abiotic stress,[51] and further root-specific investigations will

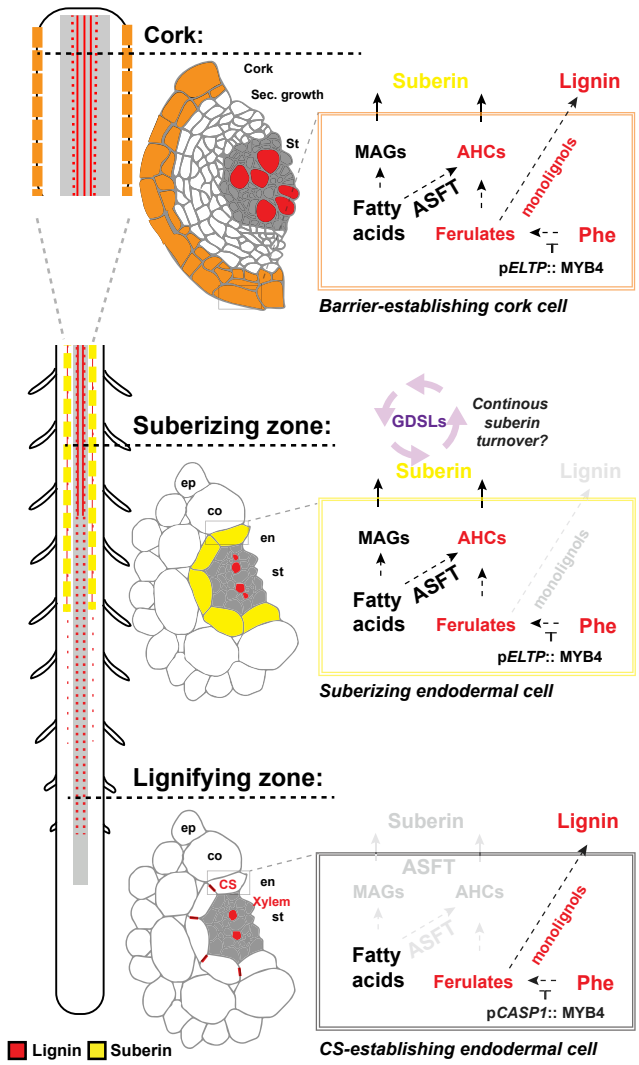

Figure 7. Spatiotemporal Coordination of Barrier-Constituent Synthesis in the Root

Synthesis of monomers necessary for root barrier construction requires the PP and fatty acid biosynthetic pathways for production of aromatic and aliphatic constituents, respectively. Based on our results, we propose a model in which, in the lignifying endodermis, the PP pathway is active and is responsible for synthesizing lignin monomers required for CS formation, whereas lignification of the xylem occurs independent via stele (St)-synthesized PP metabolites. In the suberizing zone of the endodermis, the PP pathway produces mainly ferulates, possibly through *PAL4*, which is incorporated with fatty acid metabolites via the aliphatic suberin feruloyl transferase (ASFT) into AHCs, secreted to the cell wall, and polymerized with MAGs into suberin lamellae. GDSL lipases in the cell wall degrade suberin, making the suberin depositions reflect a steady state of continuous synthesis and degradation. After secondary growth, the barrier functions of the endodermis are replaced by the cork layers. Here, the barrier consists of a complex mixture of lignin and suberin depositions that appear to be stable and represent a non-dynamic endpoint barrier, which is reflected in the role of this tissue in protecting against abiotic stresses.

likely shed light on a putative suberin-related regulatory function. Suberin constituents appear to accumulate as fatty-acid-derived constituents (Figures 5G, 6G, S4C, and S6C). Intriguingly, symbiotic associations with, for example, arbuscular mycorrhiza-forming fungi exchange photosynthates from the plant in the form of sugars and fatty acids for assimilated phosphate.[51] Because suberin deposition is decreased upon phosphate starvation,[28] it is tempting to speculate that exchange of fatty acids might correlate with suberin dynamics, and it would be interesting to explore the role of PP-derived metabolites in this communication. The GDSL motif-containing lipase cuticle destruction factor 1 (CDEF1) involved in degradation of cutin[52] has been employed as a tool to remove suberin in the endodermis,[7,13,28,40] and very recently, a range of GDSL motif-containing lipases were found to be involved in suberin dynamics.[53] This illustrates the capacity of plants for suberin catabolism by a rather simple mechanism and emphasizes that this function is likely facilitated by GDSL motif-containing lipase enzymes. Our setup with inducible repression of PP synthesis and the corresponding turnover of suberin provides an excellent platform to further unravel aspects of GDSL motif-containing lipases and suberin function in inter-species associations.

Repression of PP in the periderm leads to barrier failure, collapse of cork cells, and reduced salt tolerance, a more severe phenotype compared to any of the characterized suberin biosynthesis mutants,[22,27,54,55] emphasizing the role of the cork during abiotic stresses. Short-term repression of PP in the periderm led to release of multiple different classes of aliphatic compounds from the cork (Figure S6C). Similarly, in the endodermis, only in constitutive MYB4 expression conditions did we see specifically a release of FAs. This is not due to a different relative suberin composition of these tissues (Figure S7B) but supports that suberin dynamics are different in cork and endodermal tissues.

In conclusion, our work illustrates that genetic repressors can be used as a tool to elucidate PP pathway function in a cell-type- and tissue-specific manner. Our work provides a novel approach to affect root barrier formation and function with an unprecedented resolution and has provided intriguing insights into the complex association between PP and FA synthesis required for suberin deposition (Figure 7). The ability to control barrier formation with high resolution within tissues will help to dissect the distinct contributions of root barriers during development and in the context of specialized stress situations.

STAR★METHODS

Detailed methods are provided in the online version of this paper and include the following:

- KEY RESOURCES TABLE
- RESOURCE AVAILABILITY
  - Lead Contact
  - Materials Availability
  - Data and Code Availability
- EXPERIMENTAL MODEL AND SUBJECT DETAILS
- METHOD DETAILS
  - Molecular Cloning
  - GC-MS
  - Stainings
  - Confocal Microscopy
  - Root Suberin Coverage
  - q-PCR

- QUANTIFICATION AND STATISTICAL ANALYSIS
  - Gene List

SUPPLEMENTAL INFORMATION

Supplemental Information can be found online at https://doi.org/10.1016/j.cub.2020.11.070.

ACKNOWLEDGMENTS

We wish to thank Magdalena Marek and Colleen Drapek for their readthrough and insightful comments to the manuscript. We thank Dagmar Ripper for helping in the cork staining, as well as Robertas Ursache and Joop Vermeer for insightful discussions. The authors are grateful to the central imaging facility (CIF) at University of Lausanne for aid in image quantification and analysis. Work in the Geldner lab was supported by an ERC Consolidator grant (GA-N: 616228–ENDOFUN) and Swiss National Science Foundation grant (310030B_176399). Work in the Ragni lab is supported by the Deutsche Forschungsgemeinschaft (DFG grant RA-2590/1-2). The ORCIDs for the authors are as follows: 0000-0002-8905-0850 (T.G.A.); 0000-0001-5858-3331 (D.M.); 0000-0001-5711-3688 (J.K.); 0000-0003-2269-7390 (R.B.F.); 0000-0002-3651-8966 (L.R.); and 0000-0002-2300-9644 (N.G.).

AUTHOR CONTRIBUTIONS

T.G.A. acquired and interpreted data, conceived the research, and wrote the manuscript. D.M. conducted and analyzed GC-MS data together with J.K. R.B.F. interpreted data and contributed to writing the manuscript. D.M. and L.R. acquired the cork data. L.R. conceived the research, acquired and interpreted data, and contributed to writing the manuscript. N.G. conceived the research and contributed to writing the manuscript. All authors have approved the final manuscript and agree to be personally accountable for the individual contributions.

DECLARATION OF INTERESTS

The authors declare no competing interests.

Received: July 31, 2020
Revised: October 30, 2020
Accepted: November 30, 2020
Published: February 1, 2021

REFERENCES

1. Geldner, N. (2013). The endodermis. Annu. Rev. Plant Biol. *64*, 531–558.
2. Lee, Y., Rubio, M.C., Alassimone, J., and Geldner, N. (2013). A mechanism for localized lignin deposition in the endodermis. Cell *153*, 402–412.
3. Andersen, T.G., Barberon, M., and Geldner, N. (2015). Suberization - the second life of an endodermal cell. Curr. Opin. Plant Biol. *28*, 9–15.
4. Sitte, P. (1959). Mischkörperdoppelbrechung der Kork-Zellwände. Naturwissenschaften *46*, 260–261. https://doi.org/10.1007/BF00632301.
5. Franke, R., Briesen, I., Wojciechowski, T., Faust, A., Yephremov, A., Nawrath, C., and Schreiber, L. (2005). Apoplastic polyesters in Arabidopsis surface tissues–a typical suberin and a particular cutin. Phytochemistry *66*, 2643–2658.
6. Barberon, M., and Geldner, N. (2014). Radial transport of nutrients: the plant root as a polarized epithelium. Plant Physiol. *166*, 528–537.
7. Barberon, M., Vermeer, J.E., De Bellis, D., Wang, P., Naseer, S., Andersen, T.G., Humbel, B.M., Nawrath, C., Takano, J., Salt, D.E., and Geldner, N. (2016). Adaptation of root function by nutrient-induced plasticity of endodermal differentiation. Cell *164*, 447–459.
8. Schreiber, L. (2010). Transport barriers made of cutin, suberin and associated waxes. Trends Plant Sci. *15*, 546–553.
9. Riley, R.G., and Kolattukudy, P.E. (1975). Evidence for covalently attached p-coumaric acid and ferulic acid in cutins and suberins. Plant Physiol. *56*, 650–654.
10. Schreiber, L., Franke, R., and Hartmann, K. (2005). Wax and suberin development of native and wound periderm of potato (Solanum tuberosum L.) and its relation to peridermal transpiration. Planta *220*, 520–530.
11. Doblas, V.G., Smakowska-Luzan, E., Fujita, S., Alassimone, J., Barberon, M., Madalinski, M., Belkhadir, Y., and Geldner, N. (2017). Root diffusion barrier control by a vasculature-derived peptide binding to the SGN3 receptor. Science *355*, 280–284.
12. Fujita, S., De Bellis, D., Edel, K.H., Köster, P., Andersen, T.G., Schmid-Siegert, E., Dénervaud Tendon, V., Pfister, A., Marhavý, P., Ursache, R., et al. (2020). SCHENGEN receptor module drives localized ROS production and lignification in plant roots. EMBO J. *39*, e103894.
13. Pfister, A., Barberon, M., Alassimone, J., Kalmbach, L., Lee, Y., Vermeer, J.E., Yamazaki, M., Li, G., Maurel, C., Takano, J., et al. (2014). A receptor-like kinase mutant with absent endodermal diffusion barrier displays selective nutrient homeostasis defects. eLife *3*, e03115.
14. Racolta, A., Bryan, A.C., and Tax, F.E. (2014). The receptor-like kinases GSO1 and GSO2 together regulate root growth in Arabidopsis through control of cell division and cell fate specification. Dev. Dyn. *243*, 257–278.
15. Doblas, V.G., Geldner, N., and Barberon, M. (2017). The endodermis, a tightly controlled barrier for nutrients. Curr. Opin. Plant Biol. *39*, 136–143.
16. Ursache, R., Andersen, T.G., Marhavý, P., and Geldner, N. (2018). A protocol for combining fluorescent proteins with histological stains for diverse cell wall components. Plant J. *93*, 399–412.
17. Wunderling, A., Ripper, D., Barra-Jimenez, A., Mahn, S., Sajak, K., Targem, M.B., and Ragni, L. (2018). A molecular framework to study periderm formation in Arabidopsis. New Phytol. *219*, 216–229.
18. Campilho, A., Nieminen, K., and Ragni, L. (2020). The development of the periderm: the final frontier between a plant and its environment. Curr. Opin. Plant Biol. *53*, 10–14.
19. Almeida, T., Pinto, G., Correia, B., Santos, C., and Gonçalves, S. (2013). QsMYB1 expression is modulated in response to heat and drought stresses and during plant recovery in Quercus suber. Plant Physiol. Biochem. *73*, 274–281.
20. Thangavel, T., Tegg, R.S., and Wilson, C.R. (2016). Toughing it out–disease-resistant potato mutants have enhanced tuber skin defenses. Phytopathology *106*, 474–483.
21. Du, Y.-P., Wang, Z.-S., and Zhai, H. (2011). Grape root cell features related to phylloxera resistance and changes of anatomy and endogenous hormones during nodosity and tuberosity formation. Aust. J. Grape Wine Res. *17*, 291–297.
22. Compagnon, V., Diehl, P., Benveniste, I., Meyer, D., Schaller, H., Schreiber, L., Franke, R., and Pinot, F. (2009). CYP86B1 is required for very long chain ω-hydroxyacid and α, ω -dicarboxylic acid synthesis in root and seed suberin polyester. Plant Physiol. *150*, 1831–1843.
23. Höfer, R., Briesen, I., Beck, M., Pinot, F., Schreiber, L., and Franke, R. (2008). The Arabidopsis cytochrome P450 CYP86A1 encodes a fatty acid ω-hydroxylase involved in suberin monomer biosynthesis. J. Exp. Bot. *59*, 2347–2360.
24. Li, Y., Beisson, F., Koo, A.J., Molina, I., Pollard, M., and Ohlrogge, J. (2007). Identification of acyltransferases required for cutin biosynthesis and production of cutin with suberin-like monomers. Proc. Natl. Acad. Sci. USA *104*, 18339–18344.
25. Yang, W., Pollard, M., Li-Beisson, Y., Beisson, F., Feig, M., and Ohlrogge, J. (2010). A distinct type of glycerol-3-phosphate acyltransferase with sn-2 preference and phosphatase activity producing 2-monoacylglycerol. Proc. Natl. Acad. Sci. USA *107*, 12040–12045.
26. Yang, W., Simpson, J.P., Li-Beisson, Y., Beisson, F., Pollard, M., and Ohlrogge, J.B. (2012). A land-plant-specific glycerol-3-phosphate acyltransferase family in Arabidopsis: substrate specificity, sn-2 preference, and evolution. Plant Physiol. *160*, 638–652.

27. Molina, I., Li-Beisson, Y., Beisson, F., Ohlrogge, J.B., and Pollard, M. (2009). Identification of an Arabidopsis feruloyl-coenzyme A transferase required for suberin synthesis. Plant Physiol. *151*, 1317–1328.

28. Andersen, T.G., Naseer, S., Ursache, R., Wybouw, B., Smet, W., De Rybel, B., Vermeer, J.E.M., and Geldner, N. (2018). Diffusible repression of cytokinin signalling produces endodermal symmetry and passage cells. Nature *555*, 529–533.

29. Vermaas, J.V., Dixon, R.A., Chen, F., Mansfield, S.D., Boerjan, W., Ralph, J., Crowley, M.F., and Beckham, G.T. (2019). Passive membrane transport of lignin-related compounds. Proc. Natl. Acad. Sci. USA *116*, 23117–23123.

30. Vogt, T. (2010). Phenylpropanoid biosynthesis. Mol. Plant *3*, 2–20.

31. Koukol, J., and Conn, E.E. (1961). The metabolism of aromatic compounds in higher plants. IV. Purification and properties of the phenylalanine deaminase of Hordeum vulgare. J. Biol. Chem. *236*, 2692–2698.

32. Fahrendorf, T., and Dixon, R.A. (1993). Stress responses in alfalfa (Medicago sativa L.). XVIII: Molecular cloning and expression of the elicitor-inducible cinnamic acid 4-hydroxylase cytochrome P450. Arch. Biochem. Biophys. *305*, 509–515.

33. Mizutani, M., Ward, E., DiMaio, J., Ohta, D., Ryals, J., and Sato, R. (1993). Molecular cloning and sequencing of a cDNA encoding mung bean cytochrome P450 (P450C4H) possessing cinnamate 4-hydroxylase activity. Biochem. Biophys. Res. Commun. *190*, 875–880.

34. Teutsch, H.G., Hasenfratz, M.P., Lesot, A., Stoltz, C., Garnier, J.M., Jeltsch, J.M., Durst, F., and Werck-Reichhart, D. (1993). Isolation and sequence of a cDNA encoding the Jerusalem artichoke cinnamate 4-hydroxylase, a major plant cytochrome P450 involved in the general phenylpropanoid pathway. Proc. Natl. Acad. Sci. USA *90*, 4102–4106.

35. Smith, R.A., Schuetz, M., Roach, M., Mansfield, S.D., Ellis, B., and Samuels, L. (2013). Neighboring parenchyma cells contribute to Arabidopsis xylem lignification, while lignification of interfascicular fibers is cell autonomous. Plant Cell *25*, 3988–3999.

36. Hamberger, B., Ellis, M., Friedmann, M., de Azevedo Souza, C., Barbazuk, B., and Douglas, C.J. (2007). Genome-wide analyses of phenylpropanoid-related genes in Populus trichocarpa, Arabidopsis thaliana, and Oryza sativa: the Populus lignin toolbox and conservation and diversification of angiosperm gene families. Can. J. Bot. *85*, 1182–1201.

37. Hruz, T., Laule, O., Szabo, G., Wessendorp, F., Bleuler, S., Oertle, L., Widmayer, P., Gruissem, W., and Zimmermann, P. (2008). Genevestigator v3: a reference expression database for the meta-analysis of transcriptomes. Adv. Bioinforma. *2008*, 420747.

38. Schmid, N.B., Giehl, R.F., Döll, S., Mock, H.P., Strehmel, N., Scheel, D., Kong, X., Hider, R.C., and von Wirén, N. (2014). Feruloyl-CoA 6′-hydroxylase1-dependent coumarins mediate iron acquisition from alkaline substrates in Arabidopsis. Plant Physiol. *164*, 160–172.

39. Schalk, M., Cabello-Hurtado, F., Pierrel, M.A., Atanossova, R., Saindrenan, P., and Werck-Reichhart, D. (1998). Piperonylic acid, a selective, mechanism-based inactivator of the trans-cinnamate 4-hydroxylase: A new tool to control the flux of metabolites in the phenylpropanoid pathway. Plant Physiol. *118*, 209–218.

40. Naseer, S., Lee, Y., Lapierre, C., Franke, R., Nawrath, C., and Geldner, N. (2012). Casparian strip diffusion barrier in Arabidopsis is made of a lignin polymer without suberin. Proc. Natl. Acad. Sci. USA *109*, 10101–10106.

41. Jin, H., Cominelli, E., Bailey, P., Parr, A., Mehrtens, F., Jones, J., Tonelli, C., Weisshaar, B., and Martin, C. (2000). Transcriptional repression by AtMYB4 controls production of UV-protecting sunscreens in Arabidopsis. EMBO J. *19*, 6150–6161.

42. Fornalé, S., Lopez, E., Salazar-Henao, J.E., Fernández-Nohales, P., Rigau, J., and Caparros-Ruiz, D. (2014). AtMYB7, a new player in the regulation of UV-sunscreens in Arabidopsis thaliana. Plant Cell Physiol. *55*, 507–516.

43. Wang, X.-C., Wu, J., Guan, M.L., Zhao, C.H., Geng, P., and Zhao, Q. (2020). Arabidopsis MYB4 plays dual roles in flavonoid biosynthesis. Plant J. *101*, 637–652.

44. Roppolo, D., De Rybel, B., Dénervaud Tendon, V., Pfister, A., Alassimone, J., Vermeer, J.E., Yamazaki, M., Stierhof, Y.D., Beeckman, T., and Geldner, N. (2011). A novel protein family mediates Casparian strip formation in the endodermis. Nature *473*, 380–383.

45. Kamiya, T., Borghi, M., Wang, P., Danku, J.M., Kalmbach, L., Hosmani, P.S., Naseer, S., Fujiwara, T., Geldner, N., and Salt, D.E. (2015). The MYB36 transcription factor orchestrates Casparian strip formation. Proc. Natl. Acad. Sci. USA *112*, 10533–10538.

46. Liberman, L.M., Sparks, E.E., Moreno-Risueno, M.A., Petricka, J.J., and Benfey, P.N. (2015). MYB36 regulates the transition from proliferation to differentiation in the Arabidopsis root. Proc. Natl. Acad. Sci. USA *112*, 12099–12104.

47. Siligato, R., Wang, X., Yadav, S.R., Lehesranta, S., Ma, G., Ursache, R., Sevilem, I., Zhang, J., Gorte, M., Prasad, K., et al. (2016). MultiSite gateway-compatible cell type-specific gene-inducible system for plants. Plant Physiol. *170*, 627–641.

48. Delude, C., Fouillen, L., Bhar, P., Cardinal, M.J., Pascal, S., Santos, P., Kosma, D.K., Joubès, J., Rowland, O., and Domergue, F. (2016). Primary fatty alcohols are major components of suberized root tissues of Arabidopsis in the form of alkyl hydroxycinnamates. Plant Physiol. *171*, 1934–1950.

49. Hosokawa, M., Suzuki, S., Umezawa, T., and Sato, Y. (2001). Progress of lignification mediated by intercellular transportation of monolignols during tracheary element differentiation of isolated Zinnia mesophyll cells. Plant Cell Physiol. *42*, 959–968.

50. Alejandro, S., Lee, Y., Tohge, T., Sudre, D., Osorio, S., Park, J., Bovet, L., Lee, Y., Geldner, N., Fernie, A.R., and Martinoia, E. (2012). AtABCG29 is a monolignol transporter involved in lignin biosynthesis. Curr. Biol. *22*, 1207–1212.

51. Keymer, A., Pimprikar, P., Wewer, V., Huber, C., Brands, M., Bucerius, S.L., Delaux, P.M., Klingl, V., Röpenack-Lahaye, E.V., Wang, T.L., et al. (2017). Lipid transfer from plants to arbuscular mycorrhiza fungi. eLife *6*, e29107.

52. Takahashi, K., Shimada, T., Kondo, M., Tamai, A., Mori, M., Nishimura, M., and Hara-Nishimura, I. (2010). Ectopic expression of an esterase, which is a candidate for the unidentified plant cutinase, causes cuticular defects in Arabidopsis thaliana. Plant Cell Physiol. *51*, 123–131.

53. Ursache, R., Vieira-Teixeira, C.D.J., Tendon, V.D., Gully, K., De Bellis, D., Schmid-Siegert, E., Andersen, T.G., Shekhar, V., Calderon, S., Pradervand, S., et al. (2020). GDSL-domain containing proteins mediate suberin biosynthesis and degradation, enabling developmental plasticity of the endodermis during lateral root emergence. bioRxiv. https://doi.org/10.1101/2020.06.25.171389.

54. Domergue, F., Vishwanath, S.J., Joubès, J., Ono, J., Lee, J.A., Bourdon, M., Alhattab, R., Lowe, C., Pascal, S., Lessire, R., and Rowland, O. (2010). Three Arabidopsis fatty acyl-coenzyme A reductases, FAR1, FAR4, and FAR5, generate primary fatty alcohols associated with suberin deposition. Plant Physiol. *153*, 1539–1554.

55. Beisson, F., Li, Y., Bonaventure, G., Pollard, M., and Ohlrogge, J.B. (2007). The acyltransferase GPAT5 is required for the synthesis of suberin in seed coat and root of Arabidopsis. Plant Cell *19*, 351–368.

56. Laflamme, B., Middleton, M., Lo, T., Desveaux, D., and Guttman, D.S. (2016). Image-based quantification of plant immunity and disease. Mol. Plant Microbe Interact. *29*, 919–924.

57. Kurihara, D., Mizuta, Y., Sato, Y., and Higashiyama, T. (2015). ClearSee: a rapid optical clearing reagent for whole-plant fluorescence imaging. Development *142*, 4168–4179.

58. Berhin, A., de Bellis, D., Franke, R.B., Buono, R.A., Nowack, M.K., and Nawrath, C. (2019). The root cap cuticle: a cell wall structure for seedling establishment and lateral root formation. Cell *176*, 1367–1378.e8.

59. Schindelin, J., Arganda-Carreras, I., Frise, E., Kaynig, V., Longair, M., Pietzsch, T., Preibisch, S., Rueden, C., Saalfeld, S., Schmid, B., et al. (2012). Fiji: an open-source platform for biological-image analysis. Nat. Methods *9*, 676–682.

STAR★METHODS

KEY RESOURCES TABLE

REAGENT or RESOURCE	SOURCE	IDENTIFIER
Bacterial and Virus Strains		
Escherichia coli DH5alfa	Widely distributed	N/A
Agrobacterium tumefaciens GV3101	Widely distributed	N/A
Chemicals, Peptides, and Recombinant Proteins		
β-Estradiol (E2D.)	Sigma	Cat# E8875
Propidium Iodide (PI)	Sigma	Cat# P4864
Murashige and Skoog Basal Medium (MS)	Duchefa	Cat# M0255
Plant Agar	Duchefa	Cat# P1001.1000
CIF2	[11]	N/A
DMSO	Sigma	Cat#D8418
Xylitol (for preparing ClearSee solution)	Sigma	Cat# 87-99-0
Sodium Deoxycholate (for preparing ClearSee solution)	Sigma	Cat# D6750
Urea (for preparing ClearSee solution)	Sigma	Cat# U5378
Fluorol yellow (FY)	Santa Cruz	Cat# sc-215052
Acid lactic	VWR	Cat# 20366293
Calcofluor White	Sigma	Cat# F3543
Basic Fuchsin	Sigma	Cat# 47860
p-formaldehyde	Sigma	Cat# P6148
Piperonylic acid (PA)	Sigma	Cat# P49805
Coniferyl alcohol	Sigma	Cat# 223735
Ferulic acid	Sigma	Cat# 1270311
p-coumaric acid	Sigma	Cat# C9008
NaCl	Sigma	Cat# S3014
Cellulase,	Sigma	Cat# C2605
Pectinase	Sigma	Cat#P4716
Chloroform	Fischer Chemical	Cat#C14960/17
Methanol	Sigma	Cat#34885-M
BSTFA (bis-(N,O-trimethylsilyl)-tri-fluoroacetamide	Macherey-Nagel	Cat# 701220.110
Pyridin	Roth	Cat# CP07.1
C32 alkane	Sigma	Cat#D223107
C15 alkane	Sigma Aldrich	Cat# P3406
Critical Commercial Assays		
The Universal RNA Purification Kit	Roboklon	Cat# E3598-02
BP clonase II	Invitrogen	Cat# 11789100
LR-clonase II	Invitrogen	Cat# 11791043
ReliaPrep RNA Tissue Miniprep Kit	Promega	Cat# Z6112
PrimeScript RT Master Mix	Takara	Cat# RR036B
AMV Reverse Transcriptase Native	Roboklon	Cat# E1372-01
MESA blue	Eurogentec	Cat# RT-SYS2X-03+NRWOUB
Experimental Models: Organisms/Strains		
Arabidopsis: Col-0	Widely distributed	N/A
Arabidopsis: *pPAL1::NLS-3xVenus*	This manuscript	N/A
Arabidopsis: *pPAL2::NLS-3xVenus*	This manuscript	N/A
Arabidopsis: *pPAL4::NLS-3xVenus*	This manuscript	N/A
Arabidopsis: *pCH4::NLS-3xVenus*	This manuscript	N/A
Arabidopsis: *sgn3-3*	[11,13]	N/A

(*Continued on next page*)

Continued

REAGENT or RESOURCE	SOURCE	IDENTIFIER
Arabidopsis: *pGPAT5::mCitrin-SYP122*	[28]	N/A
Arabidopsis: *pCASP1::MYB4* in *pGPAT5::mCitrin-SYP122*	This manuscript	N/A
Arabidopsis: *pELTP::MYB4* in *pGPAT5::mCitrin-SYP122*	This manuscript	N/A
Arabidopsis: *pELTP::XVE>> MYB4-GFP* in Col-0	This manuscript	N/A
Arabidopsis: *pELTP::XVE>> MYB4* in Col-0	This manuscript	N/A
Arabidopsis: *asft-1*	[27]	N/A
Arabidopsis: *asft-2*	[27]	N/A
Arabidopsis: *pCASP1::CASP1-GFP* in Col-0	[43]	N/A
Arabidopsis: *pCASP1::MYB4* in *pCASP1::CASP1-GFP*	This manuscript	N/A
Arabidopsis: *pCASP1::MYB4* in *sgn3-3*	This manuscript	N/A
Arabidopsis: *cif1cif2* in Col-0	[11]	N/A
Arabidopsis: *pCASP1::MYB4* in *cif1cif2*	This manuscript	N/A
Arabidopsis: *pCASP1::MYB3* in *pGPAT5::mCitrin-SYP122*	This manuscript	N/A
Arabidopsis: *pCASP1::MYB7* in *pGPAT5::mCitrin-SYP122*	This manuscript	N/A
Arabidopsis: *pCASP1::MYB32* in *pGPAT5::mCitrin-SYP122*	This manuscript	N/A
Arabidopsis: *pELTP::MYB3* in *pGPAT5::mCitrin-SYP122*	This manuscript	N/A
Arabidopsis: *pELTP::MYB7* in *pGPAT5::mCitrin-SYP122*	This manuscript	N/A
Arabidopsis: *pELTP::MYB32* in *pGPAT5::mCitrin-SYP122*	This manuscript	N/A
Arabidopsis:	This manuscript	N/A
Oligonucleotides		
See Document S1	Sigma	N/A
Recombinant DNA		
P4L1r pDONR	Takara	N/A
pDONR 221	Invitrogen	Cat# 12536017
pDONR 221-MYB4	This manuscript	See Method details
pDONR 221-MYB7	This manuscript	See Method details
pDONR 221-MYB32	This manuscript	See Method details
pDONR 221-MYB3	This manuscript	See Method details
P4L1r pDONR-pELTP	[28]	N/A
P4L1r pDONR- pELTP::XVE>>	[28]	N/A
P4L1r pDONR-pCASP1	[28]	N/A
pDONR 221-gMYB4-GFP	This manuscript	See STAR Methods
P4L1r pDONR-pPAL1	This manuscript	See STAR Methods
P4L1r pDONR-pPAL2	This manuscript	See STAR Methods
P4L1r pDONR-pCH4	This manuscript	See STAR Methods
pED97	[28]	N/A
Software and Algorithms		
ZEN Black (Zen 2.3 SP1)	Zeiss	https://www.zeiss.de/corporate/home.html
Fiji/ImageJ	[56]	https://fiji.sc/)
IBM SPSS Statistics version 24-25-26	IBM	https://www.ibm.com/products/spss-statistics
CFX Maestro	BIO-RAD	https://www.bio-rad.com

RESOURCE AVAILABILITY

Lead Contact

Further information and requests for resources should be directed to and will be fulfilled by the Lead Contact, Tonni Grube Andersen (tandersen@mpipz.mpg.de).

Materials Availability

There are no restrictions to the availability of the newly generated resources except for the CIF2 peptide, which will be provided if available.

Data and Code Availability

This study did not generate any unique code. This study did not produce any unique NGS sequencing/ protein structure/microarray data.

EXPERIMENTAL MODEL AND SUBJECT DETAILS

Arabidopsis thaliana transgenic and mutant lines were used to performed experiments. For all experiments, *Arabidopsis thaliana* (ecotype Columbia 0) was used. The background and the details of each line/mutant are specified in the Key Resources Table. Seeds were kept for 2 days at 4°C in the dark for stratification, then grown at 22°C under 16 h light/8 h dark vertically on solid half-strength Murashige–Skoog (MS) medium without sucrose for all experiments except. for periderm and GC-MS analysis, in which plants were grown at 22°C under continuous light conditions.

METHOD DETAILS

Molecular Cloning

To generate endodermis specific expression constructs the genomic region of MYB3, 4 7 or 32 were amplified using specific primers (Data S1) and Gateway cloned into a pDONR221 entry vector using BP clonase II (Invitrogen) according to manufactures description. In case of MYB4-GFP, the genomic region was directly fused to GFP by overlapping PCR and inserted as one into the pDONR 221 vector. Together with previously generated P4L1r pDONR entry vectors containing either p*CASP1*, p*ELTP* or p*ELTP::*XVE>>[28], the MYB entry vectors were recombined using LR-clonase II (Invitrogen) into a fastred selection-contain destination vector (pED97). For promoter constructs p*PAL1* (4038bp) p*PAL2* (3456bp), p*PAL4* (2332 bp) and p*C4H* (2450bp) were cloned using specific primers (Data S1) into a modified gateway vector containing an attL4 R1r cassette cut with XbaI using Infusion cloning (Takara). The Promoter entry vectors were recombined using LR-clonase II (Invitrogen) into a fastred selection-contain destination vector. The final constructs were transformed into Col-0 or other backgrounds using the floral dip method[54] and selected using FastRed selection.

GC-MS

For periderm analysis, sections of ~2 cm of periderm from 20-day-old plants were collected directly from plates. Most lateral roots were cut off from the samples. For endodermis analysis, the whole root was collected if no periderm was already formed, or if the periderm was already present, only the lower portion of the root was collected. In both cases, the samples were washed by submerging three times in deionized water and carefully dried on paper towel before subsequent analysis. For suberin analysis, we followed a previously established protocol[5]. Briefly, the roots were treated with an enzymatic solution (Cellulase, Pectinase- Sigma-Aldrich, Germany) for 7 days. The solution was exchanged four times. After enzymatic treatment, unbound lipids were extracted from the roots by Soxhlet extraction with chloroform: methanol (1:1; v/v) for 2 days. The samples were dried and weighed. Consecutively, suberin was depolymerized using a 10% BF3/MeOH-based procedure[5]. In order to quantify (μg/mg sample) the suberin monomers detected by gas chromatography-coupled mass spectrometry (GC-MS), after the depolymerization, 25 μl of C32 alkane internal standard (13,5 mg/50 ml) was added in each sample. After the extraction, samples were concentrated by evaporation with N_2 until ~50 μl and posteriorly derivatized with 20 μL of BSTFA (bis-(N,O-trimethylsilyl)-tri-fluoroacetamide, Macherey-Nagel, Germany) and 20 μL Pyridin for 40 min at 70°C. For chloroform-extraction analysis, fresh samples were used. After washing with deionized-water samples were carefully weighed. In order to quantify chloroform extracts (μg/g fresh weight), 22 μL of C15 (20 μl /50 ml) was added to each sample. following this, samples were submerged in chloroform for 90 s[48]. The chloroform extracts were then evaporated with N_2 until ~50 μl. Finally, before GC-MS analysis, samples were derivatized with 20 μL of BSTFA (bis-(N,O-trimethylsilyl)-tri-fluoroacetamide, Macherey-Nagel, Germany) and 20 μL Pyridin for 40 min at 70°C. All extracts were measured using a Shimadzu TQ8040 GC-MS setup using splitless injection mode on a SH-Rxi-5SIL-MS column (30 m, 0.25 mm internal diameter, 0.25 μm film, Shimadzu Cooperation). The starting temperature was 50°C for two minutes, with an increase of 10°C per minute until 150°C, 150°C for one minute, with an increase of 3°C per minute until 310°C, and 310°C for 15 minutes. Helium was used as carrier gas with a flow rate of 0.86 mL min^{-1}. The mass spectrometer was operated in electron impact ionization (EI) scan mode. The analyses were conducted with three or five replicates. In the chloroform extractive analyses the blank was subtracted from C16 and C18 acids (all the other compounds were not detected in the blank). As C16 acid after blank subtraction was below detection it was not included in the analyses.

Stainings

For the endodermis: ClearSee staining coupled to cell wall stainings was performed as recently described in[16,57]. Briefly, plants were fixed in 3 mL 1 x PBS containing 4% *p*-formaldehyde for 1 hour at room temperature in 12-well plates and washed twice with 3 mL 1 x PBS. Following fixation, the seedlings were cleared in 3 mL ClearSee solution (10% Xylitol, 15% Sodium Deoxycholate and 25% Urea in water) under gentle shaking. After overnight clearing, the solution was exchanged to new ClearSee solution containing 0.2% Basic Fuchsin and 0.1% Calcofluor White for lignin and cell wall staining respectively. The dye solution was removed after overnight staining and rinsed once with fresh ClearSee solution. The samples were washed in new ClearSee solution for 30 min with gentle shaking and washed again in another fresh ClearSee solution for at least one overnight before observation. For quantification of Basic Fuchsin signal, recovering roots were normalized to signals from identically stained, non-PA treated Col-0 plants and plants taken directly from PA-containing plates (time point 0). For Fluorol Yellow staining of *Arabidopsis* root suberin vertically grown 5-day old seedlings

were incubated solution of Fluorol Yellow 088 (0.01%, in lactic acid) and incubated for 30 min at 70 degrees. The stained seedlings were rinsed shortly in water and transferred to a freshly prepared solution of aniline blue (0.5%, in water) for counterstaining. Following this, seedlings were washed for 2-3 min in water and transferred to a chambered cover glass (Thermo Scientific), and imaged either using Confocal laser scanning (CLSM) microscopy or a Leica DM5500 wide field microscope (GFP filtercube ex: 470 nm/40 em:525/50 bs: 500). For CLSM fluorescence, Fluorol Yellow was detected using 488 nm as excitation wavelength, and collection of emission from 500-550nm. PI assays were done as described[2] shortly, seedlings were incubated in water containing 10 μg /mL PI for 10 min and transferred into fresh water. The number of endodermal cells were scored using a Leica DM5500 wide field microscope (TX2 filtercube ex: 560 nm/40 em:645/75 bs: 595) from onset of cell elongation (defined as endodermal cell length being more than two times than width in the median, longitudinal section) until PI could not penetrate into the stele.

For the periderm: For Fluorol Yellow staining was performed as described for the endodermis except that the samples were mounted on a slide in 10% Glycerol and sample were imaged with a CLSM (Zeiss LSM880) for 3D pictures of Cork cells and with a Zeiss Axiophot epifluorescence microscope with GFP filter cube to measure the length of the different suberized zones. ClearSee coupled to Basich Fuchsin staining was performed as in the endodermis, except that after Basic Fuchsin staining, roots were washed with ClearSee solution 3times for 10 minutes and then mounted on a slide in ClearSee solution and imaged with a CLSM (Zeiss LSM880). Toluidine Blue penetration assay in the cork was performed as described for analysis in the lateral root cap[58]. Briefly, plants were collected in water in a 6-well plate, transferred in a 6-well plate containing 0.05% Toluidine Blue, incubate for 2 min and washed twice with water prior mounting then them in water on a slide. Imaging was performed straight after mounting with a Zeiss Axiophot microscope.

For the leaf: Chlorosis of leaves was measured in ImageJ[59] by measuring green channel values images as previously described[56].

Confocal Microscopy

Confocal pictures were obtained using Leica SP8 or Zeiss LSM 880 CLS microscopes.

The excitation and detection window settings to obtain signal when using a Leica SP8 were as follows: GFP (ex.488 nm, em.500–550 nm), mVenus, (ex.514 nm, em.518–560 nm). All periderm pictures were acquired with a Zeiss LSM880 with the following settings: cork autofluorescence (ex.405 nm; em. 420-460 nm), PI and Basic Fuchsin (ex.566 nm; em.570-630 nm). FY (ex.488nm, em. 490-540 nm), GFP (488nm, 490-510 nm), Venus and Citrine: (ex. 514 nm; em. 520–540 nm). 3D reconstructions and Orthogonal views of a Z stack were obtained using the ZEN Black software.

Root Suberin Coverage

Quantification of Root suberin coverage in 5-8d old root was performed as described in[7,28] Briefly, after FY stainings, the whole root is analyzed, first we measured the length of the root from the root tip to the first endodermis suberized cell (no suberin), then the distance from the first suberized cell to the point in which all endodermal cells (excluding passage cells are suberized) are suberized (patchy suberin) and then we measured the root length from that point to the hypocotyl (continuous suberin). Total root length is measured summing all 3 distances, and the relative distance of every zone is obtained dividing the distance of each zone by the total length. In the graph the mean distance of the 3 zones is plotted. The mean distance of the patchy zone is plotted on the top of the no suberin zone, and the mean distance of the continuous zones on the top of the previous developmental zone.

For older roots (from 12-old), which comprise also the periderm, the quantification is performed similarly, the only difference is that endodermis continuous suberin zone finishes at the point of the first cork cell is stained by FY, then we measure the distance from the first stained cork cell to the point in which the whole root is covered by the cork (developing periderm/cork). Finally we measure the distance from that point to the hypocotyl root junction (mature cork/periderm). Total root length is measured summing all 5 distances, and the relative distance of every zone is obtained dividing the distance of each zone by the total length. In the graph the mean distance of the 5 zones is plotted. The number of roots analyzed per genotype/treatment is mentioned in the figure legend.

q-PCR

For the *pCASP1::*MYB4 experiment: seedlings were grown on half MS without sucrose for 5 days. Only root parts (around 100 mg) were collected from each genotype and total RNA was extracted using a Trizol-adapted ReliaPrep RNA Tissue Miniprep Kit (Promega). Reverse transcription was carried out with PrimeScript RT Master Mix (Takara). All steps were done in at least triplicates and as indicated in manufactures' protocols. The qPCR reaction was performed on an Applied Biosystems QuantStudio3 thermocycler using a MESA BLUE SYBR Green kit (Eurogentech). For the *pELTP::XVE*>>MYB4-GFP experiment: plants were grown on half MS without sucrose for 19 days and then transferred in Mock or E2D supplemented half MS liquid for 48h. For the periderm: the 2 uppermost cm of the root were collected, whereas for the endodermis the lower half of the roots (without the root tip and the first 3 cm) was collected. RNA was extracted using the Universal RNA Purification Kit (Roboklon) according to the manufacturer protocol. C-DNA was synthetized using AMV Reverse Transcriptase Native (Roboklon) according to manufacturer protocol. qPCR was performed using MESA blue (Eurogentec, RT-SYS2X-03+NRWOUB) in a CFX96 Real-Time System machine (BIO-RAD). All transcripts are normalized to Clathrin adaptor complexes medium subunit family protein (AT4G24550) expression. For periderm and suberized endodermis experiments, the relative expression was calculated using CFX Maestro software (BIO-RAD) and the sample were normalized against *EF1*.Primers and gene names used for qPCR are listed in Table S1.

QUANTIFICATION AND STATISTICAL ANALYSIS

No statistical methods were used to predetermine sample size. The experiments were not randomized. Root length and the length of suberized zone was measured using imageJ / Fiji[56].

Quantification of the Propidium Iodide blockage was performed as described in[40]. All quantitative fluorescence intensities were measured using imageJ/Fiji[56] in identical optical sections of either 8- or 16-bit images with no overexposed pixels. For endodermis suberin coverage experiments, statistical analyses were performed in R-studio (ver 1.1.463) For multiple sample comparisons, a one-way ANOVA with Tukeys's post hoc (equal variance not assumed) test was performed unless otherwise stated. For the suberin root coverage quantification, statistic was performed separately for each root zone (indicate by the absence or presence of ';'';' or '' adjacent to the letters) but across all plants within one subfigure. For GC-MS and periderm experiments, statistical analyses were performed with IBM SPSS Statistics version 25 (IBM). First, the datasets were tested for the homogeneity of variances using the Levene's Test. The significant differences between two datasets were calculated using a Welch's two-tailed t test in case of a non-homogeneous variance or a Student's two-tailed t test if the variance was homogeneous. For multiple sample comparisons, a one-way ANOVA with Tamhane's post hoc (equal variance not assumed) or a Bonferroni correction (equal variance assumed) was performed unless otherwise stated. For the detailed suberin quantification of each compound/category of compound via GC-MS, statistic was performed separately for each compound/category (indicate by the absence or presence of ';''; close to letter). For the suberin root coverage quantification in old roots that comprised the periderm, statistic was performed separately for each root zone.

Gene List

The gene number of all genes mentioned in this study is presented in Table S1.